Master's thesis

NTNU
Norwegian University of Science and Technology
Faculty of Information Technology and Electrical Engineering
Department of Electric Power Engineering

Amalie Gjerdingen Jensen

Weather Models for Capturing Wind Related Failures in Probabilistic Reliability Analysis of Power Systems

Master's thesis in Energy and Environmental Engineering
Supervisor: Gerd H. Kjølle
January 2019

NTNU
Norwegian University of Science and Technology

Amalie Gjerdingen Jensen

Weather Models for Capturing Wind Related Failures in Probabilistic Reliability Analysis of Power Systems

Master's thesis in Energy and Environmental Engineering
Supervisor: Gerd H. Kjølle
January 2019

Norwegian University of Science and Technology
Faculty of Information Technology and Electrical Engineering
Department of Electric Power Engineering

NTNU
Norwegian University of
Science and Technology

Abstract

As the occurrence of extraordinary weather events such as major storms increases due to global warming, it is important to include weather data to probabilistic reliability analysis methodologies. To do so, a suitable model for implementing weather effects must be developed.

This thesis is based on the OPAL methodology and prototype which is an analytic contingency enumeration method for meshed power systems. Contingencies are chosen based on the Minimal Cut Set Method. First and second order transmission line outages are studied.
Two methods are developed to generate reliability indices from a time-series of hourly probabilities of failure for transmission lines based on historic weather data and wind-related contingencies. The aim of the methods is to reproduce results from a more complex benchmark method, while reducing computational complexity and capturing failure bunching effects.

The first method is a three weather state approximate equations method. Thi is an extension of a previously developed method which was based on a fictional case. This is altered and adapted to handle historic failure data. The second method is a timestep method.Similar to the benchmark method, the timestep method calculates unavailability at every hour of the input data-series. A MATLAB implementation to calculate reliability indices, both with and without weather impact, is developed as a part of this work.

The focus of the thesis is the effect on ENS when including weather. The studies show that the approximate equations method is most suitable for the task. A deviation to the benchmark method of 0.15 MWh/year is acheved for the system as a whole, and a deviation of 7-9% at cut set level when only studying weather-related ENS. This corresponds to a deviation of 0.3-2 % at each cut when including both weather and non-weather related ENS. The timestep method is not suitable due to overestimation increasing with weather impact.

Sammendrag

Forekomsten av ekstraordinære værfenomener som ekstremvær og store stormer øker på grunn av global oppvarming. Derfor er det hensiktsmessig å inkludere værdata til probabilistiske pålitelighets-analyse-metoder for elektriske kraftsystemer. For å gjøre det må en egnet modell for å inkludere værdata utvikles.

Denne masteroppgaven er basert på OPAL- metodikken og prototypen, som er en analytisk pålitelighets-analyse-metodikk. OPAL fokuserer på utfallskombinasjoner som fører til avbrudd for elektriske maskenett, også kalt *contingency enumeration approach*. Utfallskombinasjonene er valgt basert på Minimal Cut Set-metoden. Første- og andreordens samtidige utfall er studert.
To metoder er utviklet for å generere pålitelighetsindekser fra en tidsserie bestående av sannsynligheten for feil for hver time på overføringslinjer, basert på historiske værdata og vindrelaterte utfall. Målet med metodene er å reprodusere resultater fra en mer komplisert referansemetode, samtidig som de skal redusere kompleksiteten i modellen og fange værrelaterte feil.

Den første metoden kalles the *approximate equations method* og er en tilnærmet matematisk modell med tre værtilstander.

Metoden er en videreutvikling av en tidligere metode som var basert på fiktive data, tilpasset til å håndtere historiske feildata. Den andre metoden er kalt *timestep-metoden*. I likhet med referansemetoden beregner timestep-metoden utilgjengelighet for hver time fra tidsserien med feil-sannsynligheter. En MATLAB-implementering for å beregne pålitelighetsindekser, både med og uten værpåvirkning, utvikles som en del av dette arbeidet.

Målet med oppgaven er å modellere effekten på ILE når værdata inkluderes. Resultatene viser at the approximate equations method er mest egnet for formålet. Den avviker fra referansemetoden med 0,15 MWh/år for systemet som en helhet, og har et avvik på 7-9 % på kuttesett-nivå når en kun studerer værrelatert ILE. Dette tilsvarer et avvik på 0.3-2 % ved hvert enkelt kuttesett når det inkluderes både vær og ikke-værrelatert ILE. Timestep-metoden er ikke egnet på grunn av en økning i overestimering som følge av økt værpåvirkning.

Preface

This Master's Thesis is submitted to the Department of Electric Power Engineering at the Norwegian University of Science and Technology (NTNU) as the concluding work of my MSc in Energy and Environmental Engineering. It constitutes 30 credits, or a work load of one semester and has been conducted during the fall semester of 2018. The thesis is conducted in collaboration with SINTEF Energy Research as part of the HILP-project.

I would like to thank my supervisor Gerd H. Kjølle of SINTEF/NTNU for help, guidance and good collaboration throughout the whole period of working with this thesis. Thank you for introducing me to the interesting field of reliability analysis and providing a relevant and current project. A special thanks to Iver Bakken Sperstad of SINTEF for giving invaluable feedback throughout the semester, guiding me in the right direction and always taking the time to answer questions along the way. Also a big thanks to PhD. Candidate Erlend Sandø Kiel for help with the input data material, for having great suggestions and always having a positive attitude.

Lastly, a huge thanks to Adrian for helping me with programming, discussions whenever I was stuck and motivational support.

Oslo, January 2019
Amalie Gjerdingen Jensen

Contents

List of Figures

List of Tables

1 Introduction

1.1 Background

Modern society is highly dependent on a secure and reliable power system. With the pressing issue of reducing carbon emissions, critical infrastructure like transportation is becoming increasingly dependent on electric power. Critical communications systems which society depends on, are also dependent on energy supply. The increase in distributed generation and renewable energy sources increases the complexity of the system. This results in the utilities being highly pressured to maintain a secure supply.

Power system reliability analysis is conventionally used in power system planning to predict interruptions of supply to end-users. This has commonly been conducted using the N-1 criterion. The development of probabilistic reliability methodologies are on the rise, with international standards being developed and improvement of methodologies being conducted. With increasing complexity of the power system, rapid increase in computing power and increasing availability of sensor data from the power grid, probabilistic methods are becoming easier to utilize.

Due to climate change the occurrence of extraordinary weather events and storms are on the rise. This is a threat to the reliability of the power system. Implementation of weather data in reliability analysis is therefore necessary to improve the accuracy of the indices. This will give a more holistic and comprehensive impression of the necessary mitigation.

Several studies have been conducted and methods have been developed to implement weather data in reliability analysis. However, these methods are either based on general cases not directly based on historic weather data, like the two and three state weather model or highly input-data specific. These data specific methods are not easily transferable to other cases and input data.

1.2 Scope of Thesis

The scope of this thesis is to develop and implement weather models for reliability analysis of power systems using the OPAL Methodology. The models must handle an input time-series of hourly probabilities of component failure based on historic wind-data and wind-related failure statistics. There

are two main objectives with the weather models implementation. To study the models ability at capture failure bunching and to reproduce the indices of a more computational extensive and complex benchmark weather model by developing a weather model with reduced complexity.

The result of this thesis is a MATLAB implementation of the developed weather models and a recommendation of the most suitable weather model for the cause.

1.3 Structure of Thesis

Section 2 contains the background and theory used in the work with this thesis. The weather models are also presented here. Section 3 presents the input data-series used and the benchmark model which is to be reproduced. The work conducted in the thesis is presented here, and so is the structure of the developed MATLAB implementation. Section 4 presents and explains results. Section 5 conducts further discussion on the reasoning behind the results and compares models. In Section 6 the thesis is concluded and further work is presented.

2 Background

2.1 Reliability Analysis

The reliability of a power system is a measure of its ability to cover all end-user demand of electric power. The definition of reliability (in a bulk power electric system) from the North American Electric Reliability Counsel (NERC) is *the degree to which the performance of the elements of that system results in power being delivered to consumers with accepted standards and in the amount desired.* This definition is used by CIGRE and IEEE in [9].

To supply electric power to customers the power system must be resilient and able to withstand scheduled and unscheduled component outages and failures to avoid interruption of customer demand. There are two important aspects of defining the reliability of a power system, adequacy and security [2]. Adequacy is described as the systems ability to satisfy consumer demand and possess adequate facilities to do so. The adequacy aspect is therefore considered a steady state reliability assessment. Security is the systems ability to respond to dynamic disturbances within the system. This includes transient instabilities caused by transition between states which is ignored in the adequacy aspect. In this thesis only adequacy is considered.

Power system planning and operation to achieve a robust power system can be conducted by deterministic or probabilistic methods. The deterministic approach, which is the most utilized by transmission and distribution system operators (TSO/DSO) is the N-1 criterion. This approach secures no interruption of consumer demand if one component in the power system experiences a contingency. A contingency is an unscheduled failure of a major component in the system. If the N-1 criterion is fulfilled, any one contingency can occur.

Probabilistic methods utilizes statistical theory and methods in decision making. The power system has a stochastic behaviour which can not be perfectly predicted. However the behaviour can be estimated using statistics of previous system behaviour to locate the components most probable to experience contingencies. The methods can be used in both planning and operation of the power system. In the planning segment, analysis can be conducted to locate the combination of contingencies that cause demand interruptions and find the interruption magnitude. The results can be used to optimize resources for mitigation of critical sections of the power system. This may reduce the mitigation cost while increasing the reliability of the system. Probabilistic approaches can also

account for simultaneous contingencies of several components, which gives a better overview of the mitigation needs of the system as a whole. Planning methodologies are OPAL, MECORE, Sincal and PowerFactory [3]. This is starting to be implemented by transmission system operators(TSO) and international standards has recently been introduced [10].

Probabilistic reliability approaches can also be used in real-time operation of the power system. By utilizing real-time data of demand, supply and external influence the most probable component failure can be calculated in real-time and preventive measures to avoid load interruption can be initialized. External influences that can be monitored is weather, temperature, vegetation management, planned outages and expected repair time. By implementing probabilistic reliability methodologies in real-time, preventive measures may be conducted to reduce or avoid consequences related to contingencies. This has been studied in [11],[12]. However this is not possible to implement for all power grids with today's technology. The necessary computations are too complex and it will need an extent of real-time data input from sensors which does not exist today.

Reliability methodologies are commonly divided in two categories: Monte Carlo Simulations or analytical methods. If utilizing Monte Carlo Simulation the power system behaviour can be represented through random sampling using a Monte Carlo algorithm. This can be a good representation of the natural behaviour of the system, but is computationally extensive. Analytical methods represent the power system behaviour with a mathematical model where combinations of component failures to study are chosen. There are two main approaches for choosing failure combinations in analytical methods: state space enumeration method and contingency enumeration method. In the state space method all states causing interruptions are studied, while in the contingency enumeration approach only critical contingencies causing interruption are studied. In this thesis an analytical contingency enumeration methodology is used.

2.1.1 Hierarchical Levels

A realistic power system is large and complex. Analysis of the system as a whole is computationally extensive and time consuming. Therefore it is helpful to define the analysis in hierarchical levels(HL) as depicted in Figure 1. Level one includes generation facilities only and their capacity to supply consumer demand. The second level includes transmission facilities. Here the combination of transmission and generation contingencies are studied. This is often referred to as the

bulk transmission system. The third level also includes contingencies of components within the distribution facilities.

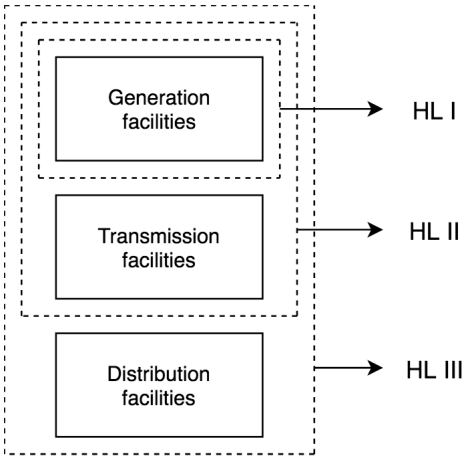

Figure 1: Hierarchical levels [2]

The system does not only consist of generators, transmission- and distribution lines. It also includes substations and substation components, interconnected tie-lines and protection systems. Reliability assessments can be conducted including all or some of these components depending on wanted depth and HL of the analysis [2]. In this thesis HLII studies are conducted.

2.2 Continuous Markov Process

The following section is based on [2], [3] and [13]. The continuous Markov process is a common representation of the behaviour of the power system in reliability analysis. This is because it is discrete in space and continuous in time. This means that a component in the system can only be in one state at a given time. The component remains continuously in the specified state until a transition takes the component to another discrete state. The system is represented as a stationary Markov process which means the expected failure and repair of components are constant in a fixed interval of time.

The conditional probability of failure and repair is considered constant, and the behaviour can be represented as an exponential distribution. Independent components can then be represented

by their failure and repair rate. A component is commonly represented by two possible discrete states, up and down. In the up-state the component is functioning as required and in the down-state the component has experienced a contingency and is in need of repair. The transition between the states are represented by the failure rate and repair rate, denoted λ and μ respectively. This is shown in Figure 2.

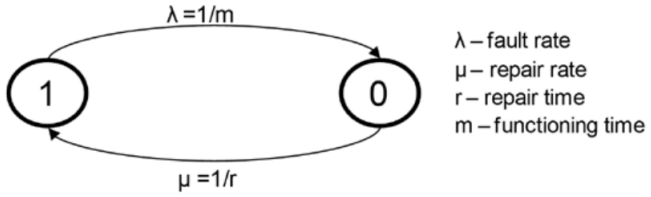

Figure 2: Two-state Markov model with the failure and repair process [3]

The transition rate of each component is calculated using statistics of previous component behaviour. This is conducted by calculating the mean time to failure (MTTF), mean time to repair (MTTR) and the mean time between failures (MTBF) based on historical data. MTBF is the sum of MTTF and MTTR. A component operation cycle is shown in Figure 3. A conceptual explanation of a transition rate is the number of transitions from a specified state to another specified state in a given time interval. This results in the failure rate $\lambda = \frac{1}{MTTF}$ and the repair rate $\mu = \frac{1}{MTTR}$, both with the unit failures/year. A mathematical proof of this is shown in [6].

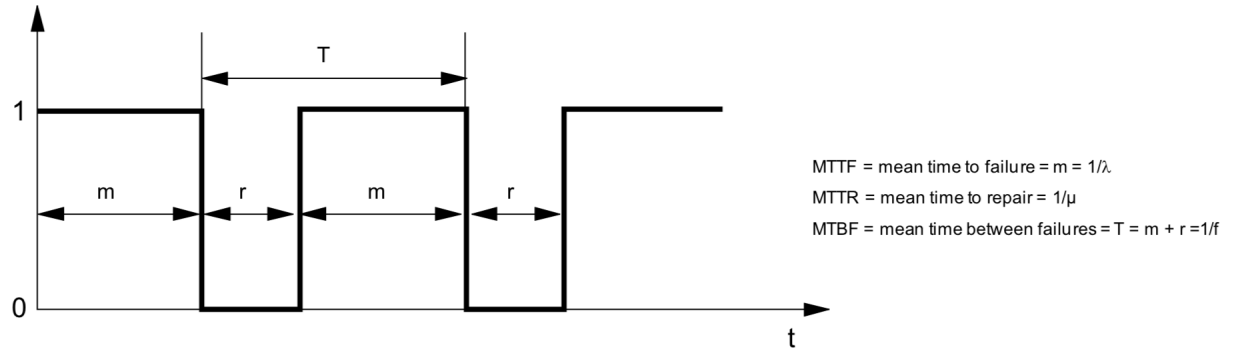

Figure 3: Component operations cycle [3]

The resultant probability of being in the up-state and down-state is shown in equation (1) and (2).

$$P_{up} = \frac{\mu}{\lambda + \mu} \qquad \text{Probability of } up \text{ state} \tag{1}$$

$$P_{0down} = \frac{\lambda}{\lambda + \mu} \qquad \text{Probability of down state} \tag{2}$$

When one component is studied there are two possible states. If the system contain two components the number of states are increased to four as shown in Figure 4 when component failures are considered independent. A modern power system consists of hundreds of crucial components and the number of states will be 2^n with n components. Computing the probability of every possible state in the system will require a huge amount of computations and have an inconveniently long computational time. It is therefore beneficial to reduce the number of states evaluated. This will be further discussed in Section 2.6.

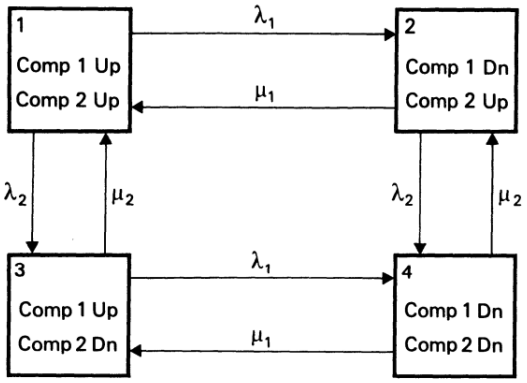

Figure 4: Two component state transition [2]

The following sections 2.3-2.8 are slightly altered sections taken from my project thesis [14].

2.3 Frequency and Duration Techniques

Frequency and duration of states are essential values when computing reliability indices. Frequency is the number of times during a given time interval we encounter a specified state. This is calculated in two ways, either with the basis of being in the state and then leaving it, or by being out of the state and entering it. E.g the frequency of encountering the *up* state is [3]:

$$f = P_1 \cdot \lambda = \text{(Probability of being in the state)}\cdot\text{(rate of departure from the state)} \tag{3}$$

OR

$$f = P_0 \cdot \mu = \text{(Probability of not being in the state)}\cdot\text{(rate of entry to the state)} \tag{4}$$

A common assumption used in most reliability studies is that MTTF equals MTBF. As the value of MTTF is often in the range of months or years between the failure of a component, the average repair time of a component is hours. This makes the average duration of the component being in down-state significantly smaller than the average duration of the component being in the up-state. The frequency of failure (f) then becomes approximate to the failure rate (λ) as shown in Equation

(5).

$$\begin{aligned} MTBF &= MTTF + MTTR \\ MTTF &>> MTTR \\ MTBF &\approx MTTF \\ \frac{1}{f} &\approx \frac{1}{\lambda} \\ f &\approx \lambda \end{aligned} \tag{5}$$

This assumption is used when calculating the unavailability (U) of a component or a minimal cut set. U is the expected number of hours a component is unavailable for operation on an annual basis. This means the expected number of hours per year a component or cut set is in down-state, in outage and in need of repair. U is also called the annual interruption duration. U is the product of expected number of failures in a given time period(f $\approx \lambda$) and the average outage duration or repair time of each failure (r) as shown in (6).

$$U = fr = \lambda r \quad \text{[hours/year]} \tag{6}$$

Equations (1)-(4) and (6) are all for single component only.

2.4 Approximate Evaluation

To ease calculation for larger and more complex systems some approximations can be made. Components can be combined to one equivalent component with equivalent parameters [13]. The expressions can also be somewhat reduced to ease computations. The approach is dependent on if the system is considered in series or parallel.

2.4.1 Series Systems

If a system consists of two components the components are considered in series if the failure of one component causes failure of the system. The series structure is shown in Figure 5. The two component parameters are then combined to create equivalent parameters for the series system as

a whole. The letter s is used to denote "series".

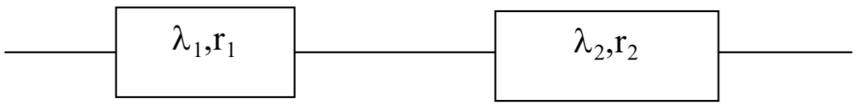

Figure 5: Series system

Probability of up-state for a two component system is:

$$P_{up} = \frac{\mu_1 \mu_2}{(\lambda_1 + \mu_1)(\lambda_2 + \mu_2)} \tag{7}$$

The probability of an equivalent one component system being in the up-state is:

$$P_{up} = \frac{\mu_s}{\lambda_s + \mu_s} \tag{8}$$

Equivalent failure rate:

$$\lambda_s = \lambda_1 + \lambda_2 \tag{9}$$

Because the probability of the up-state for the system and for one component must equal, the resultant equivalent repair time is:

$$r_s = \frac{\lambda_1 r_1 + \lambda_2 r_2 + \lambda_1 \lambda_2 r_1 r_2}{\lambda_s} \tag{10}$$

A common assumption is that $\lambda_1 \lambda_2 r_1 r_2 << \lambda_1 r_1$ and $\lambda_2 r_2$ and can be neglected. The resultant equivalent repair time is:

$$r_s = \frac{\lambda_1 r_1 + \lambda_2 r_2}{\lambda_1 + \lambda_2} \tag{11}$$

2.4.2 Parallel Systems

For a two component parallel systems the failure of one component is not affected by the failure of the other. This means that both components must fail for the system to fail. The letter p is used to denote "parallel".

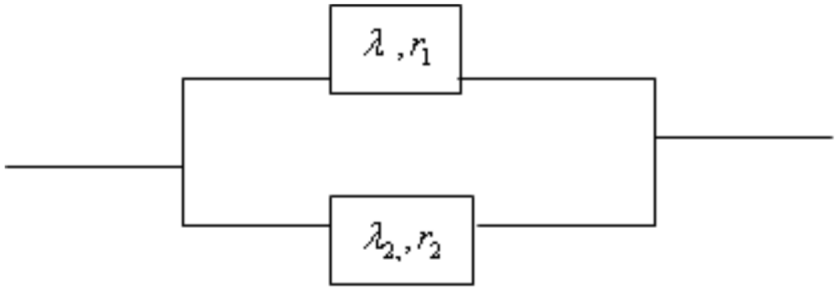

Figure 6: Parallel system

The probability of a two component system shown in Figure 4 being in the down state is:

$$P_{down} = \frac{\lambda_1 \lambda_2}{(\lambda_1 + \mu_1)(\lambda_2 + \mu_2)} \tag{12}$$

When transforming two separate components to one equivalent component the probability of the system being down is equal equation (2) as:

$$P_{down} = \frac{\lambda_p}{\lambda_p + \mu_p} \tag{13}$$

Equivalent repair time:

$$r_p = \frac{1}{\mu_p} = \frac{1}{\mu_1 + \mu_2} = \frac{r_1 r_2}{r_1 + r_2} \tag{14}$$

The probability of the down-state for the equivalent component must be equal to the down state

of the two component system:

$$\frac{\lambda_p}{\lambda_p + \mu_p} = \frac{\lambda_1 \lambda_2}{(\lambda_1 + \mu_1)(\lambda_2 + \mu_2)} \tag{15}$$

By substituting the equivalent repair time as $\mu_p = \frac{1}{r_p}$ into equation (15) the resultant equivalent failure rate is:

$$\lambda_p = \frac{\lambda_1 \lambda_2 (r_1 + r_2)}{1 + \lambda_1 r_1 + \lambda_2 r_2} \tag{16}$$

It can be assumed that $\lambda_1 r_1$ and $\lambda_2 r_2$ is a lot smaller than unity. The resultant simplified failure rate is:

$$\lambda_p = \lambda_1 \lambda_2 (r_1 + r_2) \tag{17}$$

Parameters are usually implemented with the unit per year. If annual rates are desired the failure rate expressions given above must be divided by 8760 to convert the unit to per year. This applies to both the series and parallel system. This is due to the fact that the repair time has the unit of hours and there is 8760 hours in one year.

2.5 OPAL Methodology

The OPAL Methodology is developed by SINTEF Energy Research and is a part of the SAMREL methodology [3]. SAMREL combines a market analysis [15], a contingency analysis and a reliability analysis. An OPAL prototype has been developed to perform the calculations of the contingency and reliability aspects. There exists a MATLAB and a PSSE/Python version. In this thesis the MATLAB version is used which is an implementation of the OPAL methodology consisting of a MATPOWER contingency analysis together with a reliability analysis.

OPAL is based on the contingency enumeration approach and selects contingencies based on the minimal cut set method. It is based on a continuous Markov process, frequency and duration techniques and approximate evaluation. It seeks to combine a load model, reliability model and cost model to produce delivery point reliability indices. The structure of the contingency enumeration approach used by OPAL i shown in Figure 7. Section 1 and 2 in the figure constitutes the contingency analysis and section 3 is the reliability analysis. The extent of the analysis defines the

number of simultaneous contingencies studied, also called the depth of analysis, and which power flow algorithm to be used. Operating states are defined as the system state for a given period of time, characterized by the demand and generation composition [16]. The contingency list is created, which is all possible combinations of component outages in the defined depth of the analysis. However this can be altered to reduce the number of combinations in a large power system or if something of special interest is to be studied. This can reduce the computational time significantly.

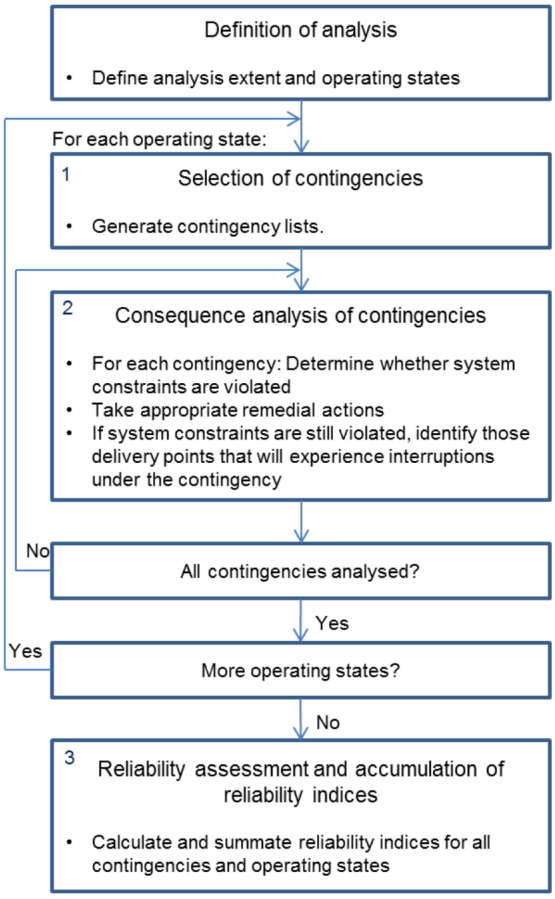

Figure 7: Flow chart of the contingency enumeration approach

The contingency list is run through an optimal power flow(OPF) algorithm to determine if any constraints of the system is violated[17]. These constraint are dependent on if the power flow al-

gorithm is AC or DC. Typical constraints are voltage or current restrictions, generation limits or overloaded transmission lines. If constraints are violated, allowed remedial actions are taken to keep the system within restriction bounds. If system constraints are still violated, one or more delivery points will be interrupted. The interrupted delivery point will be chosen based on system topology and the objective function of minimizing interruption cost. In OPAL an interruption is defined as *a situation when the total available capacity after the occurrence of a given contingency is unable to match the load at the delivery point:* [3]

$$P > SAC + LG \tag{18}$$

Where P is the demand at the given load point, SAC is system available capacity and LG is local generation [3].

When all contingencies and operating states are studied, the reliability indices are calculated. The ones commonly used are interrupted power (P_{interr}) energy not supplied (ENS), Unavailability (U) and interruption cost(IC). These are only calculated for minimal cut sets that causes interruption. Annual indices for each delivery point can also be calculated.

2.6 Minimal Cut Set Method

An essential task of an analytic reliability analysis based on the contingency enumeration approach is the selection of contingencies to be modelled. In OPAL, the Minimum Cut Set Method is used. A minimal cut set is a combination of failures that will cause load interruption if they occur, but no subset of the minimal cut set will alone cause interruption [3]. The power system can be displayed as a block diagram consisting of minimal cut sets as shown in Figure 8.

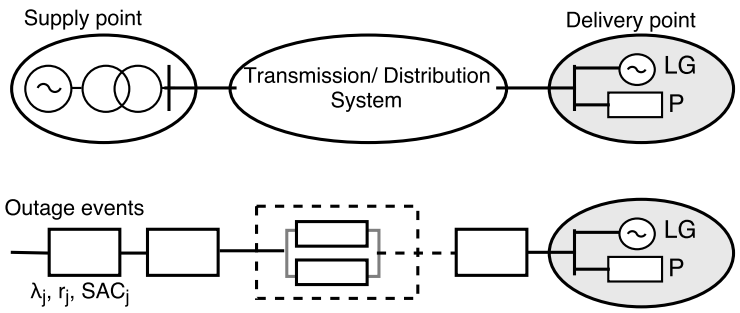

Figure 8: Reliability model for a load point using minimal cut sets [3]

Each block is represented by an unique equivalent failure and repair rate. These are calculated using the failure and repair rates for each component in the set based on equations from Section 2.4. The benefit of using the minimal cut set method is that the number of equations needed is reduced. Instead of calculating every possible state combination, only the minimal cut sets are used to calculate reliability indices. High order contingencies, which are several simultaneous contingencies, have a small probability of occurrence and may be neglected in most cases without large consequences for the calculated indices. If a cut set is denoted as first order, it contains a single contingency. A second order minimal cut set contains two contingencies to cause interruption.

2.7 Reliability Indices

Reliability indices are the results of the reliability analysis. They are a representation of the interruptions in the system and their severity. Reliability indices are calculated for every minimal cut set that causes interruption, as described in Section 2.5. The indices can be calculated for each interruption or as annual values. Annual indices for each delivery point can also be calculated. The indices are calculated using the equivalent failure rate(λ), repair time(r) and unavailability(U) calculated for each minimal cut based on equations from Section 2.3. Section 2.7.1 to 2.7.3 is taken from my project thesis [14].

2.7.1 Interrupted Power

Interrupted power is denoted P_{interr} and is the negative margin when the available capacity cannot match the load. The indicator is calculated for each delivery point and cut set. When annualized it is calculated as:

$$P_{interr,j} = \lambda_j(P - SAC_j - LG) \quad \text{[MW/interruption]} \tag{19}$$

Where j denotes the minimal cut set j, λ_j is equivalent failure rate, P is produced power, SAC is system available capacity and LG is local generation.

2.7.2 Energy Not Supplied

Energy not supplied (ENS) is the indices in focus in this report. It is as the name implies an indicator of energy not supplied at the delivery point in focus. It is calculated for each minimal cut set at each delivery point and are normally determined on an annual basis.

$$ENS_j = U_j P_{interr,j} = \lambda_j r_j P_{interr,j} \quad \text{[MWh/year]} \tag{20}$$

Where j denotes the minimal cut set j, λ_j is the equivalent failure rate, r_j is equivalent repair time and P_{interr} is the interrupted power.

2.7.3 Interruption Cost

Interruption Cost (IC) is the cost of ENS for the customer and is calculated as annual values. It is calculated for each minimal cut set, load point and operational state.

$$IC_j = c(r_j)ENS_j \quad \text{[NOK/year]} \tag{21}$$

$c(r_j)$ is the cost of the customer as a function of the duration of the fault. The function $c(r_j)$ is given as an input value in OPAL.

2.7.4 Delivery Point Indices

To calculate delivery point indices the indices of every minimal cut set causing interrupted power to the delivery point in focus is summed. This results in the annual indices for each delivery point

$$P_{interr,a} = \sum_{j=1}^{J} \lambda_j P_{interr,j} \tag{22}$$

$$ENS_a = \sum_{j=1}^{J} \lambda_j r_j P_{interr,j} \tag{23}$$

$$IC_a = \sum_{j=1}^{J} c(r_j) \lambda_j r_j P_{interr,j} \tag{24}$$

2.8 Effects of Weather

Standard reliability analysis methodologies does not account for the increased probability of failure due to weather. As shown in Figures 9-12, environmental impact is the biggest cause of failures and ENS in Norway between 2009 and 2016. With climate change, the number of storms and adverse weather situations are due to increase, and weather impact will become a greater problem. Large storms like Dagmar in 2011 [18] and the outage at Steigen, Norway in 2007 [19] will occur more frequently. Therefore it is important to include and study weather impact and High-Impact Low-Probability (HILP)-events in reliability analysis of power systems. Including weather data in planning purposes can help in building a stronger, more reliable system by achieving more accurate indices of interruption cost and ENS. This gives power system planners a more comprehensive overview of socioeconomic needs. Weather data can also help in real time operations to plan preventive and restorative actions when needed. The weather data from Figure 9-12 includes the storm Dagmar from 2011, which affects the ENS. However, this substantiates the importance of weather inclusion and its impact on ENS.

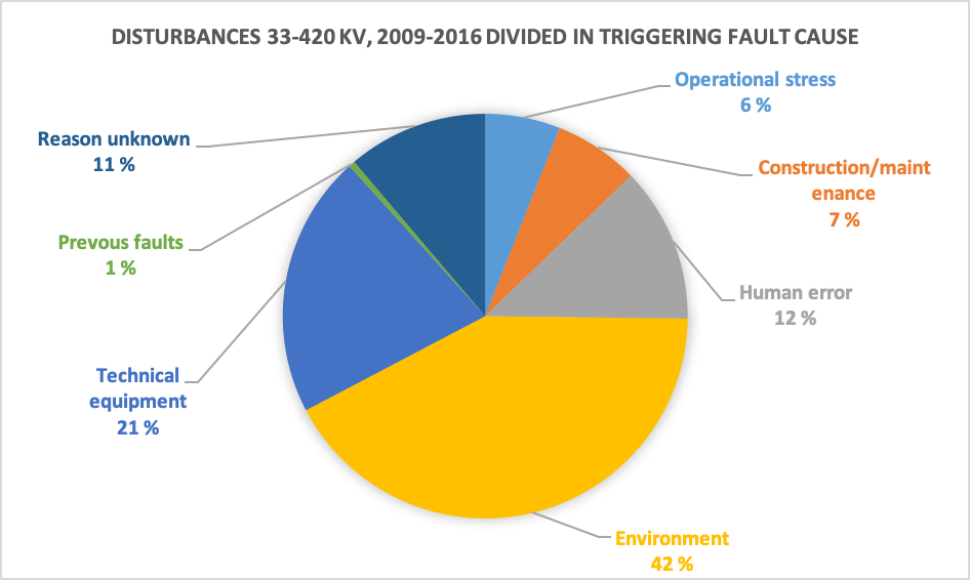

Figure 9: Fault causes, 33-420 kV, 2009-2016 [4]

Figure 9 shows the triggering fault causes in the Norwegian transmission system with voltages of 33-420 kV. The percentages are average values in the time interval 2009-2016. The largest contributor of faults are environmental impact, causing 42% of all faults. Figure 10 shows how the faults caused by the environment category from Figure 9 are grouped based on weather phenomena and other environmental causes. It shows that lightning and wind cause the largest number of interruptions.

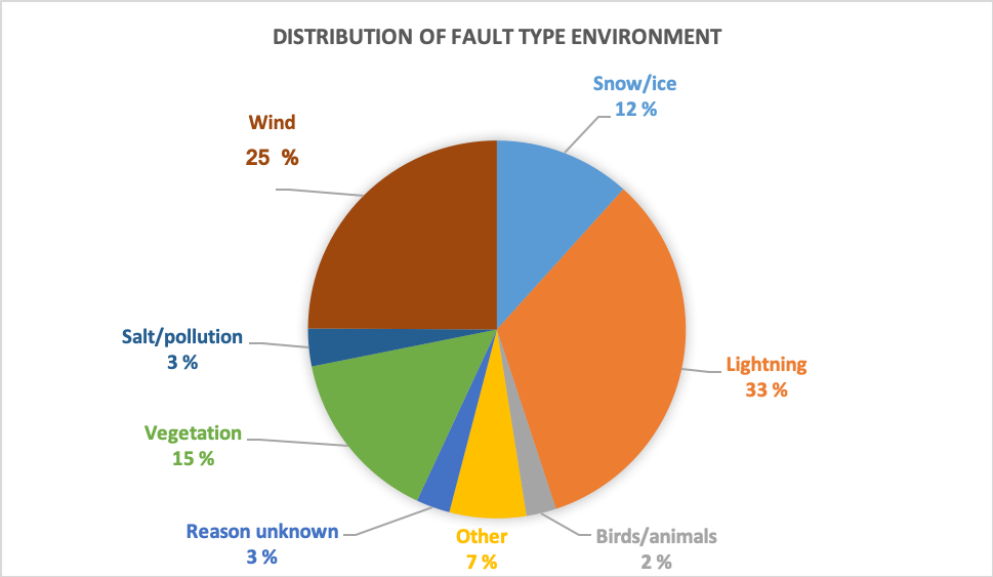

Figure 10: Distribution of fault cause in category Environment[4]

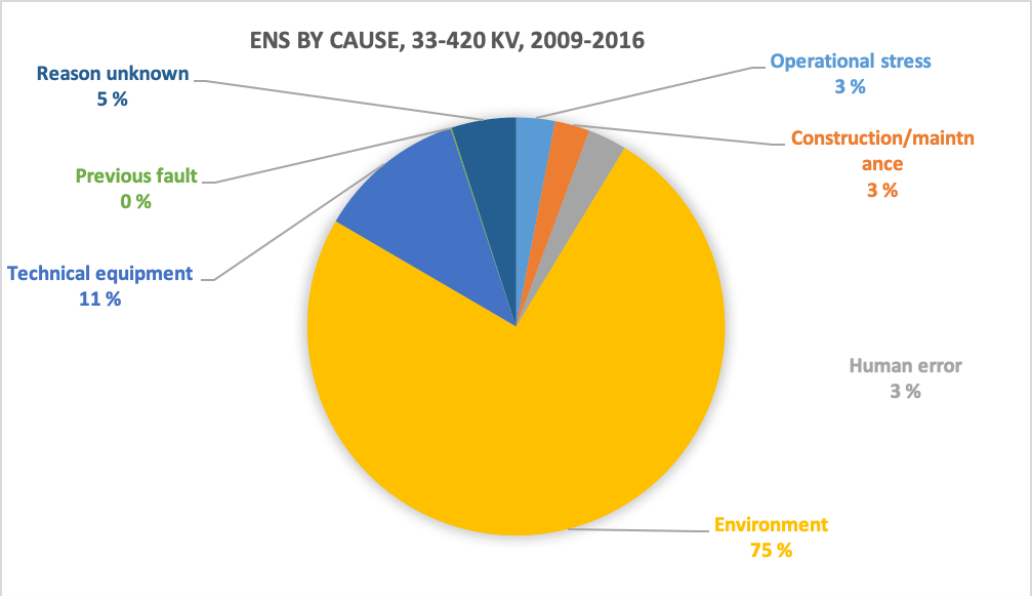

Figure 11: Cause of energy not supplied, represented by cause [4]

Figure 11 depicts which categories that affects ENS. The figure shows that 75% of ENS in the trans-

mission system in Norway are due to environmental causes in the period 2009-2016. As mentioned earlier, the storm Dagmar in 2011 is included in the data, which makes them higher than other intervals, but these are still average values of the period. In Figure 12 the category environment from Figure 11 is divided in subcategories. It shows that wind is the clearly largest environmental impact, causing 72% of ENS from the environmental category. This results in the total ENS caused by wind being $75\% \cdot 72\% = 54\%$. The reason wind is the major cause of ENS is due to association with long outage duration. Lightning causes a large number of interruptions, but the duration of contingencies are often short.

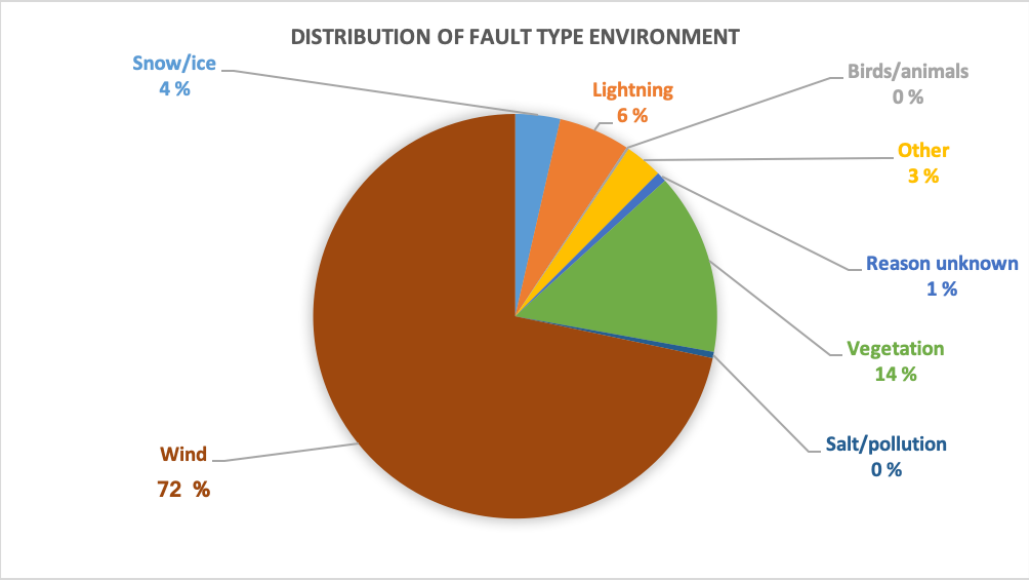

Figure 12: Distribution of energy not supplied in category Environment [4]

The total general percentage of wind-related failures are lower than 54% if studying a longer time period. In [5] all contingencies in the Norwegian power system from 1989 to 2011 has been studied. This report also implies that environmental causes is the largest contributor to ENS in this time period. The contributions within the environmental category from 1998 to 2011, missing 2006, is shown in Figure 13. Here wind is depicted in blue, lightning/thunderstorms in grey and vegetation in green. Wind is clearly a large contributor, but not as large as previous data indicates. This is probably because of the very large contributor to wind failures in 2011 caused by the storm Dagmar which highly affects the results. The total percentage of wind related failures are probably around

20%.

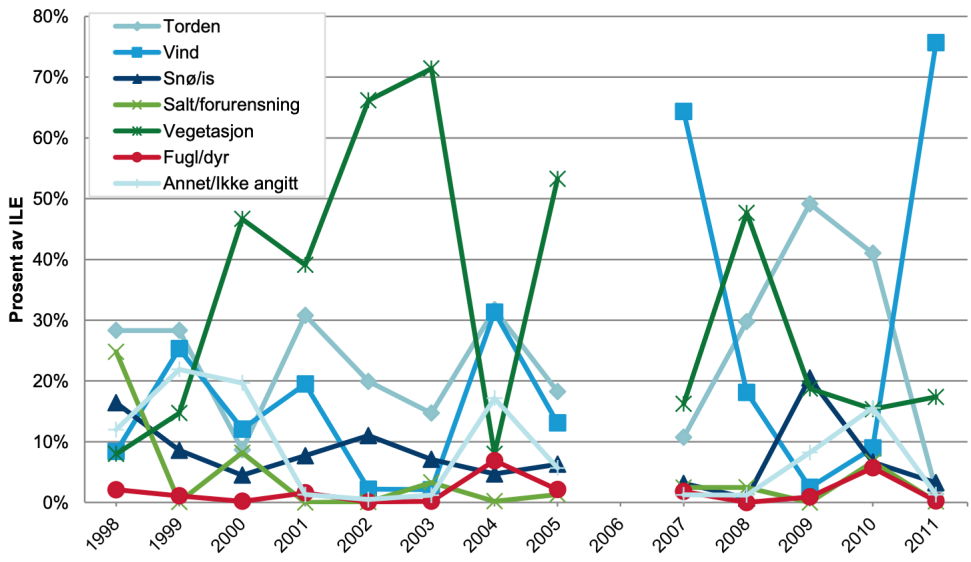

Figure 13: Percentage of ENS in category "Environment" from 1998-2011 (missing data from 2006) [5]

2.9 Capturing Failure Bunching

Failure bunching is normally referred to as the phenomenon of increased probability of overhead line failures due to increased stress on the system, i.e when exposed to bad weather [20]. This section will present some existing models developed with the purpose of capturing weather effects in reliability analysis of power systems.

The probability of failures of transmission lines are dependent on several factors. As shown in Section 2.8, weather, and wind in particular, is a large contributor to transmission line failures. The weather is continuously changing, so is the probability of system failure due to weather[1]. In most reliability analysis methodologies the failure rate, λ, is considered constant. This is highly misleading in respect to weather. By including weather dependent failure rates the resulting indices may capture failure bunching and improve the representation of the situation.

There are several developed models for inclusion of weather related contingencies in literature. The most developed and frequently used is the two- and three state weather models developed by Roy Billinton [21]. [22] also presents the use of multi-state weather models and show that the effect of increasing the number of states after 3 is small. The addition of states increases the computational time significantly. Therefore only the two- and three state model are presented here.

2.9.1 Two State Weather Model

The two state weather model utilizes the Markov approach to capture weather impact on the failure rate of components. This is done by classifying weather impact in two states; normal and adverse. If the system is in normal weather the failure rate of the system is not affected. However in adverse weather, the failure rate of the system is increased due to weather impact. The two state weather model is shown in Figure 14. [6].

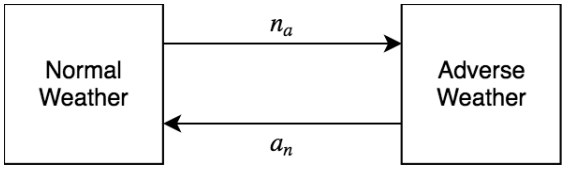

Figure 14: Two state weather model

n_a and a_n is the transition rates from normal to adverse and adverse to normal respectively. A transition rate is the expected number of transitions for a given state transition in a given period of time. Every weather state is represented by a failure and repair rate. This is λ_n and μ_n for the normal weather and λ_a and μ_a for adverse weather. This results in the following state space diagram for two components, which is a continuation of the diagram in Figure 2.

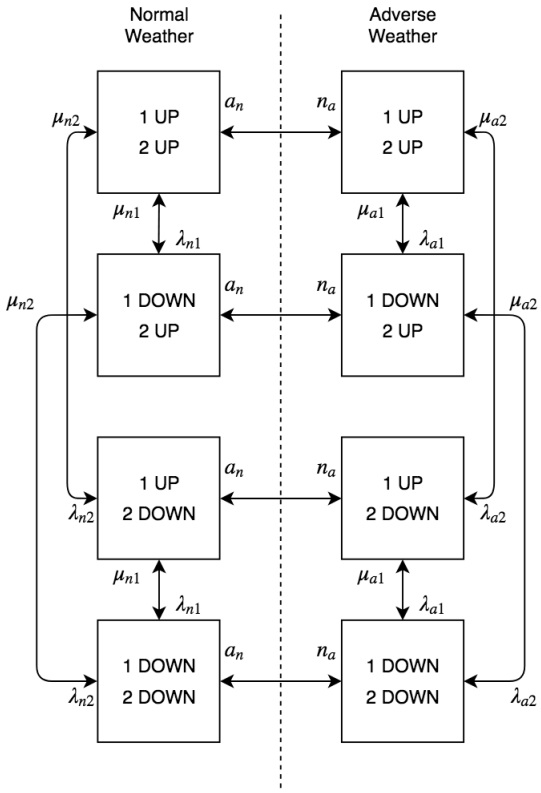

Figure 15: State space diagram with two components and two weather states[6]

2.9.2 Three State Weather Model

The three state weather model is based on the same principles as the two state model, however it includes an extreme weather state in addition to normal and adverse weather [7]. This extreme state is equivalent to the major adverse state used in literature. The extreme state is suitable for capturing HILP events which can be caused by extraordinary weather phenomenon. The effect of including the additional extreme weather state is significant as shown in [23].

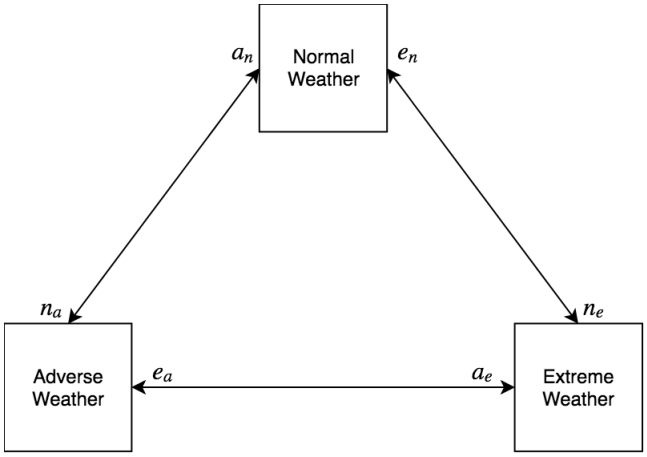

Figure 16: Three state weather model [7]

n_a, n_e, a_n, a_e, e_n and e_a is the transition rates between the weather states and can be found using historical data of weather behaviour. As with the two state model, the three weather states has a failure and repair rate for each weather state, λ_n, λ_a, λ_e and μ_n, μ_a, μ_e for normal, adverse and extreme categories respectively. The resulting state space diagram for a two component system is shown in Figure 17.

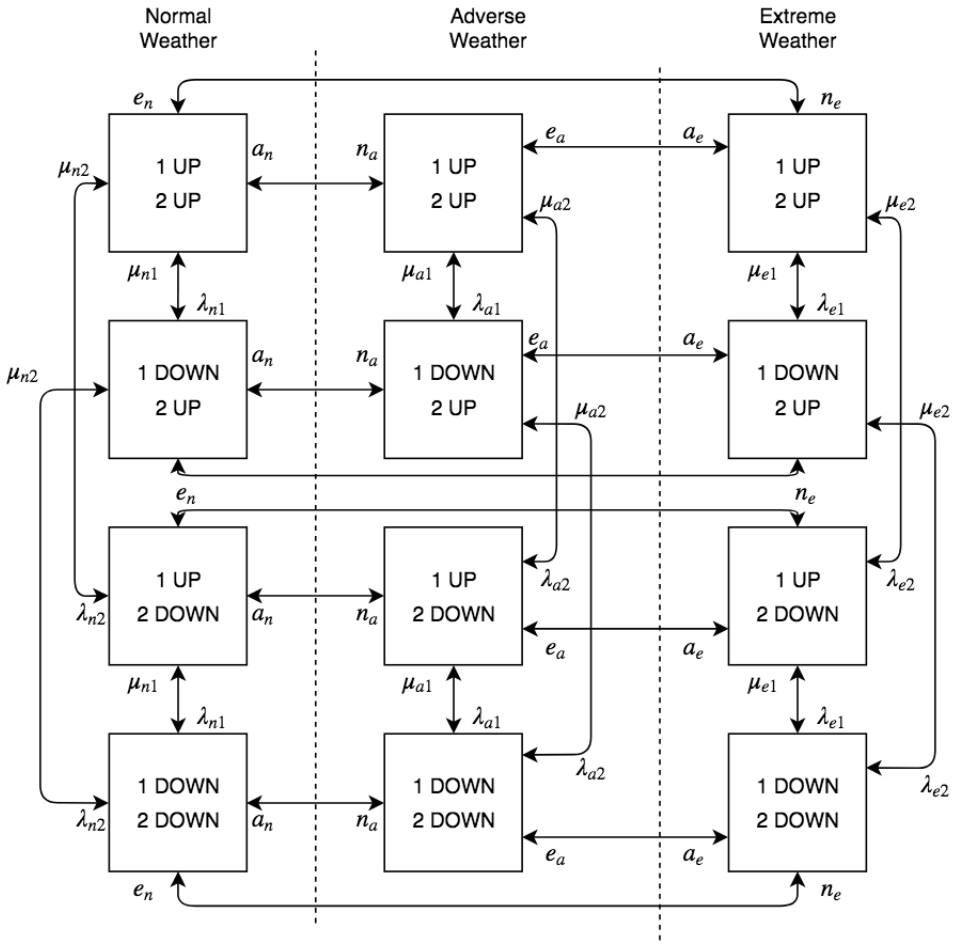

Figure 17: State space diagram of two components with three weather states [7]

As the figure shows, the number of possible states with two components and three weather categories are 12. The number of possible states in a real and complex power system will explode, and the computational time will increase significantly. Therefore it is beneficial to optimize the number of components and weather states studied to minimize the computational time and maximize the accuracy of results.

2.9.3 Other Models in Literature

Many different approaches are studied and published in literature. However these are often specifically constructed for å cause or to fit a certain input data. Hence, many of the models are not easily adapted to fit other causes. Some other weather models and studies in literature are:

[24] presents an overview of existing weather models which are divided in three categories. These are weather related component outage forecast models, outage spatial distribution prediction models and risk models. The fist model focuses on prediction of component outages using Markov processes and the two and three state Billinton weather models are mentioned. The second model uses historical data to predict outages in geographic areas. Like using machine learning algorithms to predict outages. In the third model combination of contingencies are in focus. This category represents use of state enumeration methods and Monte Carlo simulation.

[25] has developed a holistic simulation tool based on Monte Carlo simulation, weather dependent failure probabilities and contingency analysis conducted using Power Transfer Distribution Factors. [26] is developed by the same authors and describe the basis of calculating the weather dependent failure probabilities.

[27] and [28] presents an overview of important aspects in power system resilience studies. Resilience is the ability of a power system to withstand extraordinary and high-impact low-probability events. It discusses weather regions, fragility curves, restoration time and human impact. Possible mitigation for all aspects are presented. One case study is conducted in each paper. [29] by the same authors continuous to study the severity of HILP events in power systems on power system resilience. It utilizes a fragility curve model for components, OPF and sequential Monte Carlo simulations to present a resilience model for transmission lines and towers. It presents a model utilizing both temporal and regional aspects, and a case study is conducted.

[30] presents a qualitative framework for analyzing HILP events. It emphasizes the importance of understanding all uncertainties and important aspects of the analysis to maximize the detail of the result and minimize the computational time. It presents how, through the Bow-Tie model.

[31] studies two techniques of acquiring weather related failure rates of distribution lines. One is Poisson regression model. The other uses Bayesian network model and conditional probability

based of failures dependent on the weather phenomena.

[32] studies the correlation between wind speed and probability of overhead transmission line failures in the Great Britain Transmission Network. It focuses on failure rate and finds some similar correlations of weather behaviour which is studied in this thesis.

2.10 Approximate Equations Method for the Three State Weather Model

The approximate equations method is first presented in [33] for normal and adverse weather. This method is then used by R. Billinton and M.S. Grover in [34] and compared to the Markov approach. By Markov approach the method of finding the equivalent failure rate as described in Section 2.2, 2.3 and 2.4. Where every possible state combination of the system is included in the analysis, called the state space enumeration method. In [1] the model is further developed to fit the three state weather model by Billinton et.al presented in Section 2.9.2. The following section is based on the Approximate equations method presented in [1].

[1] Presents application of the two- and three state weather models both using the Markov approach and the approximate equations method to find an average failure rate of the systems. The equivalent failure rates of the two methods are compared and it can be seen that the results are similar, proving the approximate equations method being a good substitute for the Markov approach.

In this thesis the approximate equations method is a mathematical representation of the probability of second order contingencies of a two-component system based on the three state weather model. It is, as the name implies, an approximation of the Markov approach to reduce the number of calculations and computational time. This model is a suitable implementation of weather in combination with the minimal cut set method in this thesis because the depth of analysis is second order contingencies and the reliability indices are calculated for each minimal cut set separately. When studying three weather states, normal, adverse and extreme, there are nine possible failure combinations. These combinations are NN, NA, NE, AN, AA, AE, EN, EA and EE. These refer to failures in a specified weather category. The model represents the nine scenarios by approximate equations for their probability of occurrence. One important assumption in this method is that repairs can only be conducted during normal weather conditions.

Given a system with two components and three weather states the parameters are as follows:

P_n, P_a and P_e is the probability of being in the normal, adverse and extreme weather conditions respectively.

λ_{n_1} is the expected failure rate of component one in normal weather.
λ_{n_2} is the expected failure rate of component two in normal weather.
λ_{a_1} is the expected failure rate of component one in adverse weather.
λ_{a_2} is the expected failure rate of component two in adverse weather.
λ_{e_1} is the expected failure rate of component one in extreme weather.
λ_{e_2} is the expected failure rate of component two in extreme weather.
All failure rates has the unit failures per year.
r_1 and r_2 is the average repair time of component one and two respectively with the unit 1/year.

N, A and E is the expected average duration of the normal, adverse and extreme weather category respectively.

2.10.1 Transition Rates

A transition rate is the expected number of transitions from one specified state to another specified state in a specified time period. This can be explained as:

$$Transition\ rate = \frac{1}{MTTT} \tag{25}$$

With MTTT = Mean Time To Transition for the state transfer in focus. The transition rates between the weather categories are:
n_a = Transition rate from normal to adverse weather.
n_e = Transition rate from normal to extreme weather.
a_n = Transition rate from adverse to normal weather.
a_e = Transitions from adverse to extreme weather.
e_n = Transition rate from extreme to normal weather.
e_a = Transition rate from extreme to adverse weather.

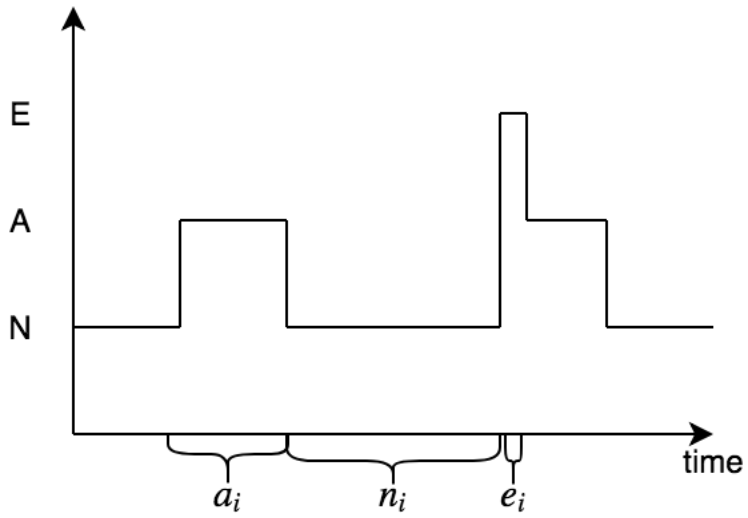

Figure 18: Transition between states

All transition rates has the unit of occurrences/year.

Figure 18 shows an example of how the weather can transition between weather states. Here N is normal, A adverse and E is extreme. n_i is the duration of normal weather before the transition to an other state for the i-th observed normal weather period. a_i is the duration of the adverse weather state for the i-th observation of adverse weather. The same concept applies to e_i. The input datasets used in this thesis consists of thousands of similar observed transitions. The MTTT is found by averaging the duration of every observed specified state before the transition to another specified state occur. This is demonstrated for the transition rate n_a in Equation 26. It should be emphasized that only duration of normal weather before the transition of adverse weather is included. Not the duration of normal weather before the transition to extreme weather.

$$n_a = \frac{1}{(\frac{\sum_{i=1}^{N} n_i}{N})} = \frac{1}{MTTT} \tag{26}$$

2.10.2 Scenarios

Every scenario contain two segments. The first one represents the failure of component one followed by the failure of component two during the repair of component one or during the duration

of the weather state in focus. Then the same probability is calculated if component two fail before component one. This is conducted to calculate all possible sequences of component failure. These are then added and multiplied with the probability of being in the initial weather state. The nine possible scenarios are:

1) First and second failure occur in normal weather(NN):

$$\lambda_1 = P_n[\lambda_{n_1}(1 - e^{-\lambda_{n_2} r_1}) + \lambda_{n_2}(1 - e^{-\lambda_{n_1} r_2})] \tag{27}$$

Where $(1 - e^{-\lambda_{n_2} r_1})$ is the probability of failure of the second component during the repair of the first component.

2) First failure occur in normal weather, and second in adverse weather(NA):

$$\lambda_2 = P_n[\lambda_{n_1}(1 - e^{-n_a r_1})e^{-\lambda_{n_2} r_1}(1 - e^{-\lambda_{a_2} A}) + \lambda_{n_2}(1 - e^{-n_a r_2})e^{-\lambda_{n_1} r_2}(1 - e^{-\lambda_{a_1} A})] \tag{28}$$

$(1 - e^{-n_a r_1})$ is the probability of the weather changing from normal to adverse during the repair time of the first component. $e^{-\lambda_{a_2} r_1}$ is the probability that the second component does not fail in the normal state during the repair of the first component. $(1 - e^{-\lambda_{a_2} A})$ represents the probability that the second component fails during adverse weather.

3) First failure occur in normal weather, the second in extreme weather(NE):

$$\lambda_3 = P_n[\lambda_{n_1}(1 - e^{-n_e r_1})e^{-\lambda_{n_2} r_1}(1 - e^{-\lambda_{e_2} E}) + \lambda_{n_2}(1 - e^{-n_e r_2})e^{-\lambda_{n_1} r_2}(1 - e^{-\lambda_{e_1} E})] \tag{29}$$

$(1 - e^{-n_e r_1})$ represent the probability that the weather changes from normal to extreme during the repair time of component one. $e^{-\lambda_{n_2} r_1}$ is the probability that the second component does not fail during the repair time of the first component. $(1 - e^{-\lambda_{e_2} E})$ represents the probability that the second component fails during extreme weather.

4) First failure occur in adverse weather, the second in normal weather(AN):

$$\lambda_4 = P_a[\lambda_{a_1}(1-e^{-a_n A})e^{-\lambda_{a_2} A}(1-e^{-\lambda_{n_2} r_1}) + \lambda_{a_2}(1-e^{-a_n A})e^{-\lambda_{a_1} A}(1-e^{-\lambda_{n_1} r_2})] \quad (30)$$

$(1-e^{-a_n A})$ is the probability of the weather changing from adverse to normal. $e^{-\lambda_{a_2} A}$ is the probability that component two does not fail during adverse weather. $(1-e^{-\lambda_{n_2} r_1})$ is the probability that the second component fail during the repair of the first.

5) Both failures occur in adverse weather(AA):

$$\lambda_5 = P_a[\lambda_{a_1}(1-e^{-\lambda_{a_2} A}) + \lambda_{a_2}(1-e^{-\lambda_{a_1} A})] \quad (31)$$

$(1-e^{-\lambda_{a_2} A})$ is the probability that the second failure occur in adverse weather.

6) First failure occur in adverse weather, the second in extreme weather(AE):

$$\lambda_6 = P_a[\lambda_{a_1}(1-e^{-a_e A})e^{-\lambda_{a_2} A}(1-e^{-\lambda_{e_2} E}) + \lambda_{a_2}(1-e^{-a_e A})e^{-\lambda_{a_1} A}(1-e^{-\lambda_{e_1} E})] \quad (32)$$

$(1-e^{-a_e A})$ is the probability of the weather to change from adverse to extreme during the adverse period. $e^{-\lambda_{a_2} A}$ is the probability that the second component does not fail during the adverse weather period. $(1-e^{-\lambda_{e_2} E})$ is the probability of the second component failing during the extreme weather period.

7) First failure occur in extreme weather, the second in normal weather(EN):

$$\lambda_7 = P_e[\lambda_{e_1}(1-e^{-e_n E})e^{-\lambda_{e_2} E}(1-e^{-\lambda_{n_2} r_1}) + \lambda_{e_2}(1-e^{-e_n E})e^{-\lambda_{e_1} E}(1-e^{-\lambda_{n_1} r_2})] \quad (33)$$

$(1-e^{-e_n E})$ is the probability that the weather changes from extreme to normal during the expected duration of the extreme weather. $e^{-\lambda_{e_2} E}$ is the probability of the second component not failing during the extreme weather. $(1-e^{-}\lambda_{n_2} r_1)$ is the probability of the second failure occur during the repair time of the first component.

8) First failure occur in extreme weather, the second in adverse(EA):

$$\lambda_8 = P_e[\lambda_{e_1}(1 - e^{-e_a E})e^{-\lambda_{e_2} E}(1 - e^{-\lambda_{a_2} A}) + \lambda_{e_2}(1 - e^{-e_a E})e^{-\lambda_{e_1} E}(1 - e^{-\lambda_{a_1} A})] \tag{34}$$

$(1 - e^{-e_a E})$ is the probability that the weather changes from extreme to adverse during the extreme weather period. $e^{-\lambda_{e_2} E}$ is the probability of the second component not failing in the extreme weather. $(1 - e^{-\lambda_{a_2} A})$ is the probability of failure of the second component during adverse weather.

9) Both failures occur in extreme weather(EE):

$$\lambda_9 = P_e[\lambda_{e_1}(1 - e^{-\lambda_{e_2} E}) + \lambda_{e_2}(1 - e^{-\lambda_{e_1} E})] \tag{35}$$

Where $(1 - e^{-\lambda_{e_2} E})$ is the probability of the second component to fail during the extreme period.

Lastly all the λ values for each possible scenario presented above is added to find the total approximate failure rate of the system. Because every scenario is multiplied with the respective probability of being in the original state, the failure rates are weighed and can be simply added.

$$\lambda_{approx} = \lambda_1 + \lambda_2 + \lambda_3 + \lambda_4 + \lambda_5 + \lambda_6 + \lambda_7 + \lambda_8 + \lambda_9 \tag{36}$$

2.10.3 Input Parameter Correlation

[1] states some important correlations between the input parameters of the method. Given the transition rates of the system other parameters like the average duration of weather, probability of weather states and weather related failure rates can be calculated.

$$N = \frac{1}{n_a + n_e} \tag{37}$$

$$A = \frac{1}{a_n + a_e} \tag{38}$$

$$E = \frac{1}{e_a + e_n} \tag{39}$$

Equation (37)-(39) say that the average duration in each weather state is one over the average time it resides in that state before leaving it. This is a reasonable statement which is exemplified by the calculation of one transition rate in Equation (40). When calculating the average duration for the system using the three state weather model, the situation is more complex because a state can be left by two possible transitions, as shown in Equation (37)-(39). However the logic behind the correlation is still valid.

$$Average\ duration = \frac{1}{transition\ rate} = \frac{1}{\frac{1}{MTTT}} = MTTT \tag{40}$$

From the transition rates the probability of residing in either weather state can also be calculated as:

$$P_n = \frac{e_a a_n + e_n a_n + e_n a_e}{D} \tag{41}$$

$$P_a = \frac{e_a n_a + e_a n_e + e_n n_a}{D} \tag{42}$$

$$P_e = \frac{n_a a_e + n_e a_n + n_e a_e}{D} \tag{43}$$

Where $D = e_a n_a + m_a n_e + e_a a_n + n_a a_e n_e a_n + n_e a_e + e_n a_n + e_n a_n + e_n a_e + e_n n_a$.
From the acquired information of transition rates, average duration and probabilities it should be possible to calculate the weather dependent failure rates. However this is not described for the three state model in [1]. For the two state model, the equations are presented in Equation (44)-(46).

$$\lambda_{avg} = \lambda_n(\frac{N}{N+A}) + \lambda_a(\frac{A}{N+A}) \tag{44}$$

This results in the λ at each weather state to be:

$$\lambda_n = \lambda_{avg}\frac{N+A}{N}(1 - F_a) \tag{45}$$

$$\lambda_a = \lambda_{avg}\frac{N+A}{A}F_a \tag{46}$$

Where λ_{avg} represents the total average failure rate of the component. F_a is the ratio of faults occurring in adverse weather. When calculating the failure rate for the three weather state model it would be natural to believe a similar approach is reasonable. This is presented and used in [35]

and shown in equation (47)-(50).

$$\lambda_{avg} = \lambda_n \frac{N}{N+A+E} + \lambda_a \frac{A}{N+A+E} + \lambda_e \frac{E}{N+A+E} \tag{47}$$

Which would result, by following the same principal, in the weather dependent failure rates as:

$$\lambda_n = \lambda_{avg} \frac{N+A+E}{N}(1 - F_a - F_e) \tag{48}$$

$$\lambda_a = \lambda_{avg} \frac{N+A+E}{A} F_a \tag{49}$$

$$\lambda_e = \lambda_{avg} \frac{N+A+E}{E} F_e \tag{50}$$

Here F_e is the ratio of failures occurring in the extreme weather category. However, this is not a correct method due to the extreme category being misrepresented. This will be further discussed in Section 3.3.

[21] presents a different method of calculating the failure rates of each weather category shown in equation (51)-(53). Here the average failure rate is multiplied with the ratio of failures in each category and divided by the probability of being in the weather state in focus.

$$\lambda_n = \lambda_{avg} \frac{(1-F)}{P_n} \tag{51}$$

$$\lambda_a = \lambda_{avg} \frac{F(1-F_e)}{P_a} \tag{52}$$

$$\lambda_e = \lambda_{avg} \frac{F \cdot F_e}{P_e} \tag{53}$$

Here, F is the ratio of "bad weather" which is the sum of the ratio of failures in adverse and extreme weather; $F = F_a + F_e$.

2.11 The Timestep Method

The timestep method is a method disregarding the categorization of weather, and calculating unavailability(U) at each time step of a time series. Unavailability is the probability of a component being unavailable i.e in the down-state. The data-series does not require categorization into weather

categories based on probability of failure due to weather phenomena. This results in no data lost due to categorization of weather states. The method assumes a constant repair time(r) which needs to be a integer.

The time series used in this thesis contain the hourly probability of failure due to wind. This is a unit less probability, but can be interpreted as the hourly failure rate λ_t with the unit probability of failure per hour [1/hour]. The objective is to calculate the probability of the component being in the down-state in every time step. To do this, the probability of the component having already experienced a previous failure and being in outage at the time step in focus must be included. This can be done in two ways:

$$p(U_t) = 1 - \prod_{t=1}^{-r} (1 - p(\lambda_t)) \tag{54}$$

$$p(U_t) = \sum_{t=1}^{-r} p(\lambda_t) \tag{55}$$

Equation (54) calculates the probability of the component being in the up-state, also called the availability for the time step in focus and all previous time steps within the given repair time. These are then multiplied to calculate the availability for the time-section in focus. This results in the probability of the component having experienced a previous failure and being in repair at the time-step in focus to be included. Next the unavailability, or the probability of the component being in the down-state of the time-step in focus, is calculated by $U = 1 - availability$. This is the correct approach according to probability theory making certain the probability of component outage or component up-state never exceeds unity. However the hourly probability of failure of an component is very small. In this thesis the repair time is constant at 11 hours and in that time period, with the data set used, the summation of the probability of failure for 11 hours will never exceed unity. Therefore a simplification of summing the probabilities as shown in Equation (55) can be used.

This method is similar to the normal calculation of the unavailability as shown in Equation (6). In Equation (6) a constant failure rate is multiplied with a repair time. In the timestep method, a time-series of varying probabilities of failure, or failure rates for every hour. These failure rates has the unit 1/hour. When these fluctuating failure rates over the timespan of the repair time are summed, the same concept as in (6) is followed. When the sum of the hourly failure rate and the repair time is multiplied, the resultant unavailability becomes unitless. This allows for the multi-

plication of unavailabilies of separate lines to produce the equivalent unavailability of a cut set as shown in Equation (56). This multiplication is viable whether Equation (54) or (55) is used.

$$U_{eq,t} = p(U_t)_1 \cdot p(U_t)_2 \tag{56}$$

To be able to use this equivalent unavailability to calculate reliability indices, the expression must equal the equivalent unavailability when using the standard Equation (6), and match the unit of [hours/year]. This is achieved by summing the equivalent unavailability of every hour in the time series divided by the number of years. In the case in this thesis with a span of 25 years the calculation will be as shown in Equation (57). In this equation the unit calculation of the summation is also shown, assuming constant U_eq, t to exemplify and show that the unit notation matches.

$$U_{eq} = \frac{\sum_{t=1}^{T}(U_{eq,t})}{years} \approx \frac{U_{eq,t}[1] * 24[\frac{hours}{day}] * 365[\frac{days}{year}] * 25[years]}{25[years]} = U_{eq}[\frac{hours}{years}] \tag{57}$$

The timestep method can only calculate unavailability for repair times which are integers. This causes a problem if the repair time of the system is a decimal number. To adjust for this, the method must be slightly altered. A weighing constant is introduced to include the remaining repair time element shown in Equation (58). Where r_{actual} is the actual repair time of the system, and $r_{integer}$ is the integer repair time used in Equation (54) and (55). The weighing factor is included as shown in Equation (59) and (60).

$$w = \frac{r_{actual}}{r_{integer}} \tag{58}$$

$$p(U_t) = 1 - w \cdot \prod_{t=1}^{-r}(1 - p(\lambda_t)) \tag{59}$$

$$p(U_t) = w \cdot \sum_{t=1}^{-r} p(\lambda_t) \tag{60}$$

3 Method

3.1 The Data Material

The data material used in this thesis is a time-series of hourly probabilities of failure of an overhead transmission line due to wind. The time-series contain failure probabilities for a time span of 25 years and is developed for 12 overhead transmission lines located in Norway.[1]

The failure probabilities are developed according to the method in [26], however all wind-related transmission line failures are included, not only those caused by wind speeds above 15 m/s. Historical average failure rates due to wind in an area and actual contingencies due to wind of selected transmission lines are used in a Bayesian updating scheme to develop line specific failure rates. Next a historic wind-exposure measure is produced for each line segment. The historic wind-data implemented is hourly wind speeds from a 1-km grid around each line-segment. This historic wind-data is collected from [37].

The line-specific failure rates and the historic wind-exposure measure is combined to construct a fragility curve for each line-segment. A fragility curve is the cumulative log-normal distribution function of the failure probability of a line with the wind-exposure as the input variable [26]. This is used to find the probability of failure for each segment for every hour given the historic wind-data. The probability of failure for each line-segment can be considered as in series to find the probability of failure for the line as a whole. Lastly the probability of every line is estimated based on this series calculation with the limitation that the results of the series calculation must be consistent with the total number of line failures found through the Bayesian updating scheme. This results in a time-series of hourly probabilities of failure for each line. The time-series with hourly probabilities of failure for line 1 is shown in Figure 19.

[1] The data is developed by and used in collaboration with PhD candidate Erlend Sandø Kiel and the method is presented in [36].

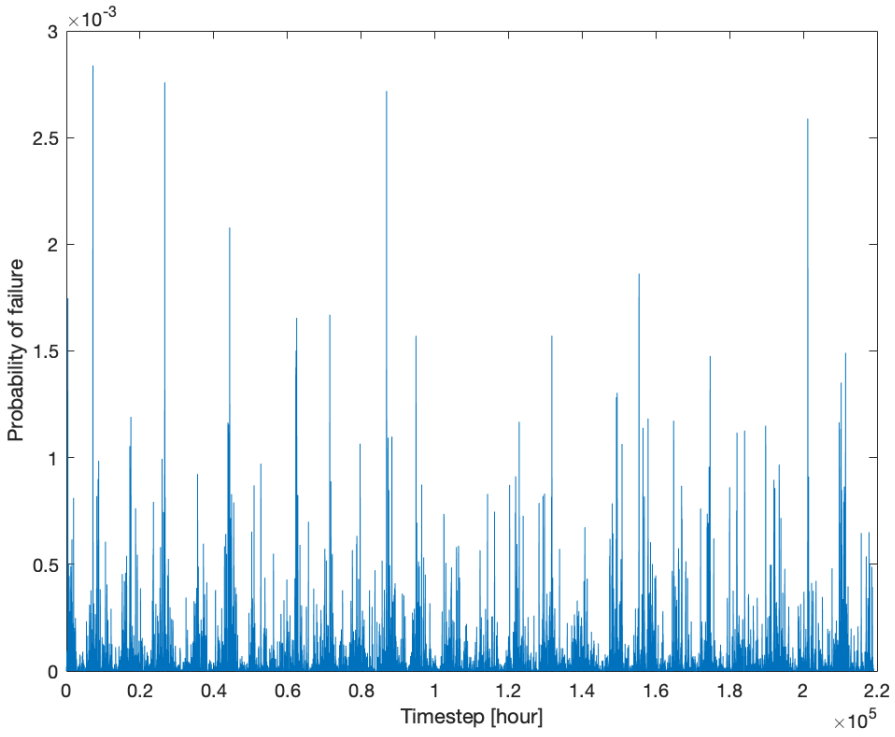

Figure 19: Probability of failure time-series for line 1

3.1.1 Benchmark Method

Throughout the results section all methods will be compared to benchmark results. These ENS results are calculated for the RBTS system utilizing the method presented in [36] with the same input line failure probabilities as presented above.

The aim of this method is to calculate an unavailability time-series of a line based on the probability of failure time-series and probabilistic outage duration. Outage duration is defined the time from a contingency occur to the component is again ready to operate, also called the repair time. In the benchmark method an outage duration curve is constructed to represent the probability of the component being in the down-state a given number of hours after the occurrence of a contingency. This curve is constructed based on historic failure data from the Norwegian transmission grid from the database FASIT [38]. This data is used to find the log-normal probability density function(PDF)

where some measures are conducted to assure that the mean and variance of the original data are preserved. The cumulative distribution function(CDF) of the time-period in focus from the PDF is utilized to find the survival function of the outage data for each line. The survival function is the probability of the component being in the down-state a given number of hours after the contingency. Lastly the probability of unavailability is calculated by combining the survival function and the probability of failure at each time-step. An inflation factor due to an assumed outage duration cut off is also included. The resultant unavailability is then used to calculate reliability indices. A more detailed description of the benchmark method can be found in [36]. All reliability indices of the benchmark method can be found in the Appendix.

The benchmark method is similar to the timestep method described in Section 2.11. However the outage duration or repair time is considered constant at 11.42 hours. This outage duration equals the average outage duration calculated in the benchmark method. The simplifications in the timestep method reduces computational time significantly, but also reduces the accuracy of results. This will be further discussed.

3.2 Roy Billington Test System

The test system used to analyze the models are the Roy Billington Test System (RBTS) [8]. This is a power system developed for educational purposes to study the adequacy aspect of reliability analysis. It contains 6 buses in total, with 4 PQ load buses and 2 PV generation buses. There are a total of 9 lines containing both single lines and lines on a common tower or right of way.

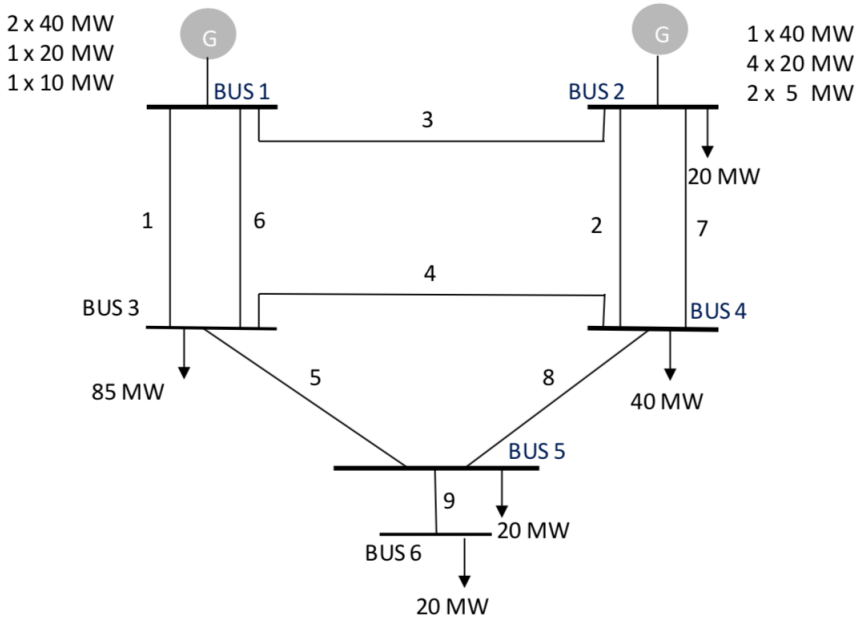

Figure 20: Roy Billington Test system [3] based on [8]

All generation units are placed at bus 1 and bus 2, where the generation is thermal and hydro powered respectively. Their ratings are shown in Figure 20. Generators are not affected by increased wind speeds and are therefore considered 100% reliable in this analysis. The total generation capacity is 240 MW. The delivery point demand is also depicted in the figure with their respective consumption and placement. They are considered price independent. The annual peak demand of the system is 185 MW, and this demand is price-independent.

The voltage level of the system is 230 kV and line data is shown in Table 1. Where R, X and B are the resistance, impedance and susceptance respectively. λ is the permanent outage rate with unit outages per year. Transient failure rates for the lines are not included in the analysis due to the fact that transient failures does not affect the adequacy of the system because of short duration. r is the average repair time. It should be noted that the repair time is altered from the original RBTS data to match the average repair time from the historical input data. This is to achieve consistency in results.

Line nr	From Bus	To Bus	R	X	B	λ	r [h]	length [km]
1,6	1	3	0.0342	0.18	0.0212	1.5	11.4209	75
2,7	2	4	0.1140	0.6	0.0704	5	11.4209	250
3	1	2	0.0912	0.48	0.0564	4	11.4209	200
4	3	4	0.0228	0.12	0.0142	1	11.4209	50
5	3	5	0.0228	0.12	0.0142	1	11.4209	50
8	4	5	0.0228	0.12	0.0142	1	11.4209	50
9	5	6	0.0228	0.12	0.0142	1	11.4209	50

Table 1: Line input data

Contingencies of circuit breakers, buses and transformers may occur and cause consequences for the reliability of the system. However, in this analysis these are assumed to be 100% reliable. Buses and transformers are not significantly affected by increased wind speeds and are therefore not considered. The circuit breakers may be affected, however inclusion of circuit breakers are considered to complicate the computations more than it contributes to the illustration of increased wind.

There are several costs related to the operation of a power system. In this analysis the generation cost and interruption cost are included. The generation cost is the fuel- and operating expenses of the generators. This is used to find the optimal generation dispatch. Generation cost used in the analysis is shown in Table 2. These are from the RBTS model [8] with a small alteration. The hydro powered generators and 40 MW thermal generators originally have equal cost. This might result in variations of the optimal dispatch of generation in each simulation. To avoid this, equal generation costs are slightly increased resulting in no equal cost.

Bus	Type	MW	Cost
Bus 1	Thermal	40	1.2
Bus 1	Thermal	40	1.21
Bus 1	Thermal	20	1.225
Bus 1	Thermal	10	1.25
Bus 2	Hydro	40	0.05
Bus 2	Hydro	20	0.051
Bus 2	Hydro	20	0.052
Bus 2	Hydro	20	0.053
Bus 2	Hydro	20	0.054
Bus 2	Hydro	5	0.055
Bus 2	Hydro	5	0.056

Table 2: Generation cost

The interruption cost is the cost of the customer if desired delivery point demand is not met. The OPF algorithm in the simulation tool has an objective function to minimize total interruption cost when prioritizing delivery points and distributing power flow. Therefore the input interrupted cost is important for the resultant reliability indices. The delivery point interruption costs are taken from the "Priority order policy" from [39] and are shown in Table 3.

Load point	Bus	Priority order	IC
LP 1	Bus 2	1	9.6325
LP 2	Bus 3	5	4.3769
LP 3	Bus 4	3	8.0267
LP 4	Bus 5	2	8.6323
LP 5	Bus 6	4	5.5132

Table 3: Interruption Cost

3.2.1 Pairing of Lines from Dataset

It is desirable to pair the real transmission lines from the time-series data set with comparable lines in the RBTS system to get the most realistic results. This was conducted by studying the distance between lines, line length and weather correlation of lines, shown in Table 4 and Figures 21 and 22. The original dataset consist of 12 lines in a random order. 9 of these lines are chosen to be paired with the RBTS system.

Line nr	1	2	3	4	5	6	7	8	9	10	11	12
Length (km)	9	14	37	16	16	42	4	44	90	102	86	56

Table 4: Line Length

Line	1	2	3	4	5	6	7	8	9	10	11	12
1	0	6	48	44	44	20	37	17	281	97	36	74
2	6	0	54	49	49	24	43	13	279	95	30	70
3	48	54	0	21	21	33	17	59	316	130	84	118
4	44	49	21	0	0	25	9	49	323	137	79	118
5	44	49	21	0	0	25	9	49	323	137	79	118
6	20	24	33	25	25	0	19	25	300	115	54	94
7	37	43	17	9	9	19	0	44	314	128	73	110
8	17	13	59	49	49	25	44	0	287	105	33	76
9	281	279	316	323	323	300	314	287	0	187	256	212
10	97	95	130	137	137	115	128	105	187	0	79	44
11	36	30	84	79	79	54	73	33	256	79	0	44
12	74	70	118	118	118	94	110	76	212	44	44	0

Figure 21: Distance between center of lines in km (By Erlend Sandø Kiel)

Line	1	2	3	4	5	6	7	8	9	10	11	12
1	1	0,712699	0,620179	0,570906	0,563263	0,715008	0,493695	0,545662	0,043992	0,530564	0,463336	0,631321
2	0,712699	1	0,604366	0,572066	0,577906	0,687933	0,453936	0,511023	0,061168	0,498375	0,482791	0,58892
3	0,620179	0,604366	1	0,733058	0,715957	0,695551	0,594258	0,482702	0,077896	0,552328	0,592042	0,681858
4	0,570906	0,572066	0,733058	1	0,991445	0,721522	0,710575	0,605721	0,145527	0,571693	0,611827	0,638353
5	0,563263	0,577906	0,715957	0,991445	1	0,710874	0,701383	0,582133	0,127867	0,552419	0,587441	0,617024
6	0,715008	0,687933	0,695551	0,721522	0,710874	1	0,581626	0,616217	0,0903	0,570901	0,553517	0,696948
7	0,493695	0,453936	0,594258	0,710575	0,701383	0,581626	1	0,509847	0,074098	0,498329	0,503494	0,550584
8	0,545662	0,511023	0,482702	0,605721	0,582133	0,616217	0,509847	1	0,234544	0,587929	0,76965	0,604191
9	0,043992	0,061168	0,077896	0,145527	0,127867	0,0903	0,074098	0,234544	1	0,194683	0,247119	0,171559
10	0,530564	0,498375	0,552328	0,571693	0,552419	0,570901	0,498329	0,587929	0,194683	1	0,735692	0,899651
11	0,463336	0,482791	0,592042	0,611827	0,587441	0,553517	0,503494	0,76965	0,247119	0,735692	1	0,731607
12	0,631321	0,58892	0,681858	0,638353	0,617024	0,696948	0,550584	0,604191	0,171559	0,899651	0,731607	1

Figure 22: Weather correlation between center of lines (By Erlend Sandø Kiel)

Figure 21 show the distance between transmission lines evaluated from the center point of each line. Figure 22 show the correlation between the probability of failure due to wind for each line. 1 denotes total correlation and 0 is no correlation. Firstly, line number 9 was disregarded as it is located in another climate zone and has no correlation to other lines. Next it can be seen that line 4 and 5 has no distance between and almost perfect correlation of failure probabilites due to wind. This means that the lines are on a common tower and is chosen to represent line 1 and 6 in the RBTS system due to short length.

RBTS	Dataset
1	4
2	10
3	11
4	3
5	6
6	5
7	12
8	2
9	8

Table 5: Resultant line pairing relationship

The correlation of failure probability between line 10 and 12 is strong at almost 0.9, and distance between the lines are small considering total length. Therefore line 10 and 12 are chosen as line 2 and 7 in RBTS which have the same right of way. Next, line 11 is chosen to represent line 3 in RBTS due to its length and because it has a decent correlation to all adjacent lines, especially line 10 and 12.

Due to short line lengths of line 1 and 7 with 9 km and 4 km respectively, they were considered non-representative of the RBTS system. The remaining lines are then line 2, 3, 6 and 8 from the time-series data set and are closely the same length. From Figure 22 it can be seen that line 6 has the best overall correlation to other lines and are chosen to represent RBTS line 5. It is also observed that line 2 has a better correlation to other lines than line 8 and 3, and is therefore chosen to represent line 8 in the RBTS system. Lastly it is observed that line 3 has a better overall correlation to other lines than line 8 and is therefore chosen as RBTS line 4 which leaves line 8 to represent RBTS line 9. This results in the line pairing shown in Table 5.

The excluded lines from the data-set are line 1, 7 and 9. When using the developed code for this thesis and the input file "$f\_lines\_rbts.csv$", the lines are arranged in the correct order. With line 1 in the data-set matching line 1 in the RBTS and so on. Therefore no active adjustments are needed to implement this input data-set when running the simulations.

3.3 Validation of the Approximate Equations Method

The approximate equations method presented in Section 2.10 need to be validated to ensure correct implementation of the method. This can be done by reproducing results presented in [1], which

will also substantiate the statements in the paper. An MATLAB implementation was built based on Equation (27)- (36) to conduct the validation.

[1] calculates approximate equivalent failure rates for a two-component system with different degrees of weather impact and three weather states. The input data used to recreate the paper are shown in Table 6 and 7. Table 7 shows the transition rates where the vertical weather state axis shows the "from" state, and the horizontal is the "to" state. For all input parameters, except the probabilities, it is important to convert the unit to per year. This results in all transition rates multiplied by 8760 and weather duration and repair time is divided by 8760 which is the number of hours in one year.

Parameter	Value
λ_{avg}	2
P_n	0.989875
P_a	0.010011
P_e	0.000114
N	195.54 hours
A	1.9995 hours
E	1 hour
r_1	7.5 hours
r_2	7.5 hours

Table 6: Input data for method validation

	N	A	E
N	-	$\frac{1}{200}$	$\frac{1}{8760}$
A	$\frac{1}{2}$	-	$\frac{1}{8760}$
E	$\frac{1}{2}$	$\frac{1}{2}$	-

Table 7: Input transition rates for method validation

[1] does not specify the equations used to calculate the weather dependent failure rates for the three weather state model. From literature two possible methods were found. One is the method presented in [35] with formulas presented in equation (47)-(50) from now called the duration method. The second possible method is the one presented in [21] and equations (51)-(53), from now called the probability method. In both methods, the ratio of bad weather was increased from 0% to

100%. This percentage includes both adverse and extreme weather. In all scenarios 5% of the bad weather occur in the extreme category. E.g for the case of 50 % bad weather this results in 47.5 % in adverse and 2.5 % in extreme.

For the duration method the resultant failure rates are shown in Table 8. Here F is the percentage of failures occurring in bad weather, which is the sum of failures in adverse and extreme states.

F	λ_n	λ_a	λ_e
0	2.03068	0	0
10	1.82761	18.86516	1.98535
20	1.62454	37.73031	3.97071
30	1.42148	56.59547	5.95606
40	1.21841	75.46062	7.94141
50	1.01534	94.32578	9.92676
60	0.81227	113.19093	11.91212
70	0.60920	132.05609	13.89747
80	0.40614	150.92124	15.88282
90	0.20307	169.78640	17.86817
100	0	188.65156	19.85353

Table 8: Weather dependent failure rates using duration method

It can be seen that the failure rate of the extreme category is lower than the adverse category, which is illogical. In [1] one example of failure rates are given. This is when 5 % of the total failures occur in the extreme category, corresponding to the 100 % case in Table 8. In the paper the weather dependent failure rate of extreme weather is $\lambda_e = 876$. This is a huge deviation from the results of the duration method, which implies that the method is erroneous.

Another way of testing if the results are correct is by calculating λ_{avg} for each step which should equal 2, as defined in the article. This is done using equation (61) [1]. As seen in Table 9, none of the calculated average failure rates are equal 2, which is a confirmation of the method being invalid. The calculated average is decreasing due to the missing effect of the extreme weather category. The resultant calculation of λ_{approx} is shown in Table 26 in the Appendix. It also shows that the authors of [1] did not use this method in their calculations.

$$\lambda_{avg} = P_n\lambda_n + P_a\lambda_a + P_e\lambda_e \tag{61}$$

F	λ_{avg}
0	2.01012
10	1.99819
20	1.98627
30	1.97434
40	1.96241
50	1.95049
60	1.93856
70	1.92663
80	1.91471
90	1.90278
100	1.89085

Table 9: Resultant λ_{avg} for the duration method

By utilizing the probability method it was possible to calculate the correct weather dependent failure rates for each state which are shown in Table 10. When calculating λ_{avg} based on the calculated failure rate and Equation (61) it is equal 2 in every state of F. The resultant λ_{approx} is shown in Table 11, and is almost exactly equal to the benchmark results from [1]. This proves that the probability method was used to calculate the weather dependent failure rates in [1].

F	λ_n	λ_a	λ_e
0	2.02046	0	0
10	1.81841	18.97912	87.71930
20	1.61637	37.95825	175.43860
30	1.41432	56.93737	263.15789
40	1.21227	75.91649	350.87719
50	1.01023	94.89561	438.59649
60	0.80818	113.87474	526.31579
70	0.60614	132.85386	614.03509
80	0.40409	151.83298	701.75439
90	0.20205	170.81211	789.47368
100	0	189.79123	877.19298

Table 10: Weather dependent failure rates, probability method

F	λ_{approx}	Benchmark	Deviation
0	0.00691	0.00691	0
10	0.00846	0.00846	0
20	0.01366	0.01366	0
30	0.02248	0.02247	0.00001
40	0.03488	0.03488	0
50	0.05086	0.05085	0.00001
60	0.07037	0.07036	0.00001
70	0.09339	0.09338	0.00001
80	0.11990	0.11988	0.00002
90	0.14986	0.14985	0.00001
100	0.18326	0.18325	0.00001

Table 11: λ_{approx} and deviation of reconstruction and original paper

By finding the missing formulas and information used in this method it has been possible to recreate the results. This proves that the created MATLAB implementation is correct. It also increases the credibility of the approximate equations method being a good supplement for the more extensive Markov approach.

3.4 Implementation of Time-series to the Approximate Equations Method

The input parameters must be found to apply the approximate equations method with the time-series data-set. All inputs are correlated as shown in Section 2.10.3, and a starting point must be chosen. Here the starting point is chosen to be the probability of residing in each weather state. This probability is taken from the works of R. Billinton [7][1][23]. It is based on the assumption that the average weather duration is 200 hours in normal, 2 hours in adverse and 1 hour in extreme. This results in the following input probability of weather states:

P_n	P_a	P_e
0.989875	0.010011	0.000114

Table 12: Input probability of weather states

The probabilities are used to categorize every hour in the time-series of each line into weather states based on their magnitude. The 98.99% lowest percentile of failure rates are categorized as normal weather, the next 1% are categorized as adverse weather and the highest thousandth is sorted as

extreme weather. This is shown in Figure 23. I.e the extreme category represents approximately the one hour each year with the highest probability of component failure. In the figure this is the last vertical section of the curve. The failure rate of each state is calculated by averaging all failure rates of the state. These are the weather dependent failure rates λ_n, λ_a and λ_e

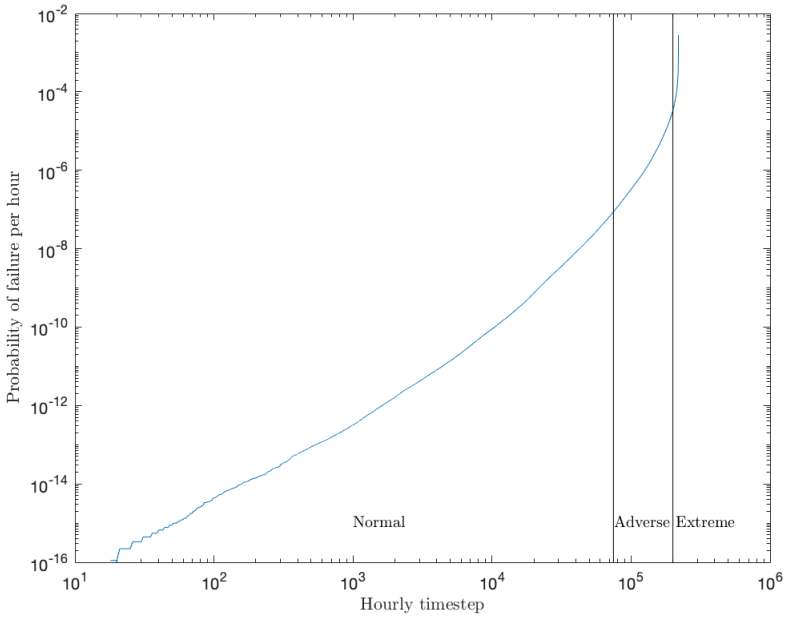

Figure 23: Loglog representation of the categorization of failure probability

The boundary values between weather states are used to find the transition rates between each states and the average duration of every state between transitions. The time-series is looped through and every change between states and the number of hours the system resided in the previous state before the transition is recorded. This data is saved in the duration matrix, and the placement in the matrix is based on the weather states involved in the transfer. An example of this matrix is shown in Table 13. Where the "from" states are on the vertical axis and "to" on the horizontal.

	N	A	E
N	-	[]	[]
A	[]	-	[]
E	[]	[]	-

Table 13: Duration matrix structure

Initially the transitions rates were calculated by following the concept of MTTT from Equation (25). The MTTT was calculated from the matrix and used to find the transition rates. The transition rates were then used to calculate the average duration of a weather state using Equations (37)-(39). In the input time-series data some transitions are rare, especially transitions between the extreme and normal weather states. By further examination of the recorded data in the duration matrix, these rare transitions occur in periods of unstable, and fast-changing weather. In almost all occurrences of transitions from the normal to extreme state, the duration of normal weather before the transition to extreme is one hour. When using the transition rates to calculate the average duration of each weather state using Equation (37) the transition from normal to adverse and normal to extreme is equally weighed. This is despite there being hundreds of observations of normal to adverse and one or two from normal to extreme. This results in the average duration of the normal weather state being shorter than what is the actual situation.

Problems arise with the transition rates due to the scarcity of some transitions too. Scenario 3 in the approximate equation method, where the first failure occur in normal weather and second in extreme weather, is highly over-represented. This is due to the transition rate, and the probability of this transition to occur, being illogically large because the observed duration of normal weather before a transfer to the extreme state is short.

A new approach for calculating transition rates and average duration of weather states were implemented. Using the duration matrix, the average duration of each state is calculated directly from the matrix. This reduces the necessary computations and resolves the misrepresentation of transition rates. E.g for the average duration of the normal weather state:

$$N = \frac{sum\ of\ hours\ in\ n_a + sum\ of\ hours\ in\ n_e}{total\ number\ of\ observed\ transitions\ from\ normal\ weather}$$

Here the number of all hours in the normal state before a transition to the adverse state, and the number of all hours in the normal state before the transition to the extreme state is added.

This is then divided by the number of total observed transitions from the normal weather state. The transition rates are now found through the actual number of observed transitions and not the MTTT. The correct unit of transition rates are occurrences per year. Hence, the number of all observed transitions from a specified state to another specified state are divided by the number of years in the time-series. E.g calculation of the transition rate n_a:

$$n_a = \frac{Number\ of\ observed\ transitions\ from\ normal\ to\ adverse}{Number\ of\ years\ in\ time-series}$$

This change in calculation of the transition rates and average duration results an improvement in how the approximate equations method represents the actual behaviour of the weather. The method presented in [1] is correct if there are enough observations of every transition in the system. When implemented on real historic weather data, the infrequent transitions get misrepresented. When implementing and testing this change, the contribution from the scenarios in the approximate equations method are following the same pattern as the contributions found when recreating the original paper. By using this method the relationship between the input parameters presented in Section 2.10.3 are no longer valid, however due to the changes the method is implementable using historic weather data.

3.5 Contingency Analysis

The contingency analysis is not affected by weather impact. It is therefore conducted separately and the results are used as input to the code developed in this thesis. The OPAL prototype version 2.1, last updated November 2018, is used.

3.5.1 Input

In the OPAL prototype, the MATLAB file *contanalysis_RBTS_Benchmark.m* is used to run the simulation. The excel input file is *RBTS_Benchmark.xls* placed in the subfolder *CaseStudies*.

The line, generation and load data presented in Figure 20 and Tables 1, 2 and 3 are used as input data to the contingency analysis. The base MVA is set to 100 and the analysis depth includes second order branch outages. Generators, buses and protection system is considered reliable and are not included as possible contingencies. The common mode functionality is not activated.

The detailed description of line ratings and voltage limits can be found in [8].

The power flow algorithm chosen is DC optimal power flow(OPF). This is to emphasize the contributions to ENS caused by weather impact to the adequacy of the system. By assuming lossless lines using DC, fewer parameters affect results, and essential changes in the system due to failure bunching are easier to analyze. When running AC power flow more minimal cut sets are causing interruption an must be studied. These extra cut sets often have an interrupted power of less than 0.5 MW. It is considered sufficient to study the weather impact using DC power flow.

In the excel sheet "actions" in *RBTS_benchmark.xls* the corrective actions settings are set. The activated corrective actions are *allow_islanding*, *distr_slack*, *opf*, *all_pot_swing*, *collapse_infeasible*, *distr_by_max_cap*. Not all these are used when running DC OPF, however it allows for successful use of the file for AC OPF without any changes. The number of iterations are set to 10.

3.5.2 Results

The contingency analysis return several results. The one used further to calculate the reliability indices is the struct *cont_results*. From this struct the SAC matrix and the full version of the component out matrix is used. The component out matrix shows the contingency list that causes interruption. Every component in each cut set is denoted either 1 or 0. If a component is denoted 1 it is experiencing a failure, if 0 it is operating normally. The SAC matrix shows the system available capacity for every cut set in the contingency list. The rows in the component out matrix and in the SAC matrix represent the same cut set. Both matrixes returned from the contingency analysis and used as input to the reliability analysis can be found in the Appendix.

The contingency analysis can be conducted in any simulation tool which provides it. However the code structure developed in this thesis require a SAC and component out matrix on the format presented in the Appendix.

3.6 MATLAB Implementation

SINTEF Energy research has developed a simulation tool for contingency and reliability analysis [40]. This tool is complex and not easily altered. To be able to easily add and test alternative methods of calculating reliability indices including weather impact a new reliability analysis implementation was constructed in MATLAB as a part of this thesis. This code is based on the assumption of constant repair rates and inclusion of 1st and 2nd order minimal cut sets. In the RBTS system, only parallel cut sets cause delivery point interruption, therefore only equivalent equations for parallel systems are included.

3.6.1 OPAL Methodology Including Average Weather

The structure of the code calculating reliability indices based on the OPAL methodology is shown in Figure 24. The standard calculation of reliability indices, based on the OPAL methodology, can be simulated both with and without weather impact. If standard reliability analysis without weather is wanted, the indices are calculated as described in Sections 2.3, 2.4.2 and 2.7. If average weather is desired the structure of the code is as described in Figure 24.

The script Main.m is common for all described methods, and the desired weather model for calculation is chosen here. The input parameters, λ_{rbts}, delivery point demand and repair time is defined. The results from the contingency analysis is loaded to workspace.

Next the `LP_cutset` function finds the minimal cut sets at every delivery point in the system. This function compares the demand of each delivery point with the system available capacity matrix matching a combination of component failures from the component out matrix. If a combination results in energy not supplied at the delivery point, the transmission lines experiencing a failure and is in the down-state, is registered as a cut set. All cut sets at each delivery point are then compared to see if any cut set is a subset of another cut set. If this is the case, the largest cut set is removed due to it not being minimal.

Equivalent indices of each cut set is calculated in `equivalents_weather.m`. The indices calculated are equivalent failure rate, repair time, interrupted power and unavailability. When average weather is included, the equivalent failure rate is calculated as shown in Figure 24. Here the sum

of the failure probabilities for a line from the input time-series is divided by the number of years of the input data to find the average contribution of wind per year. This average is added to λ_{rbts} for the line in focus. The average weather impact is added to each line separately before the equivalent failure rate is calculated using Equation (16).

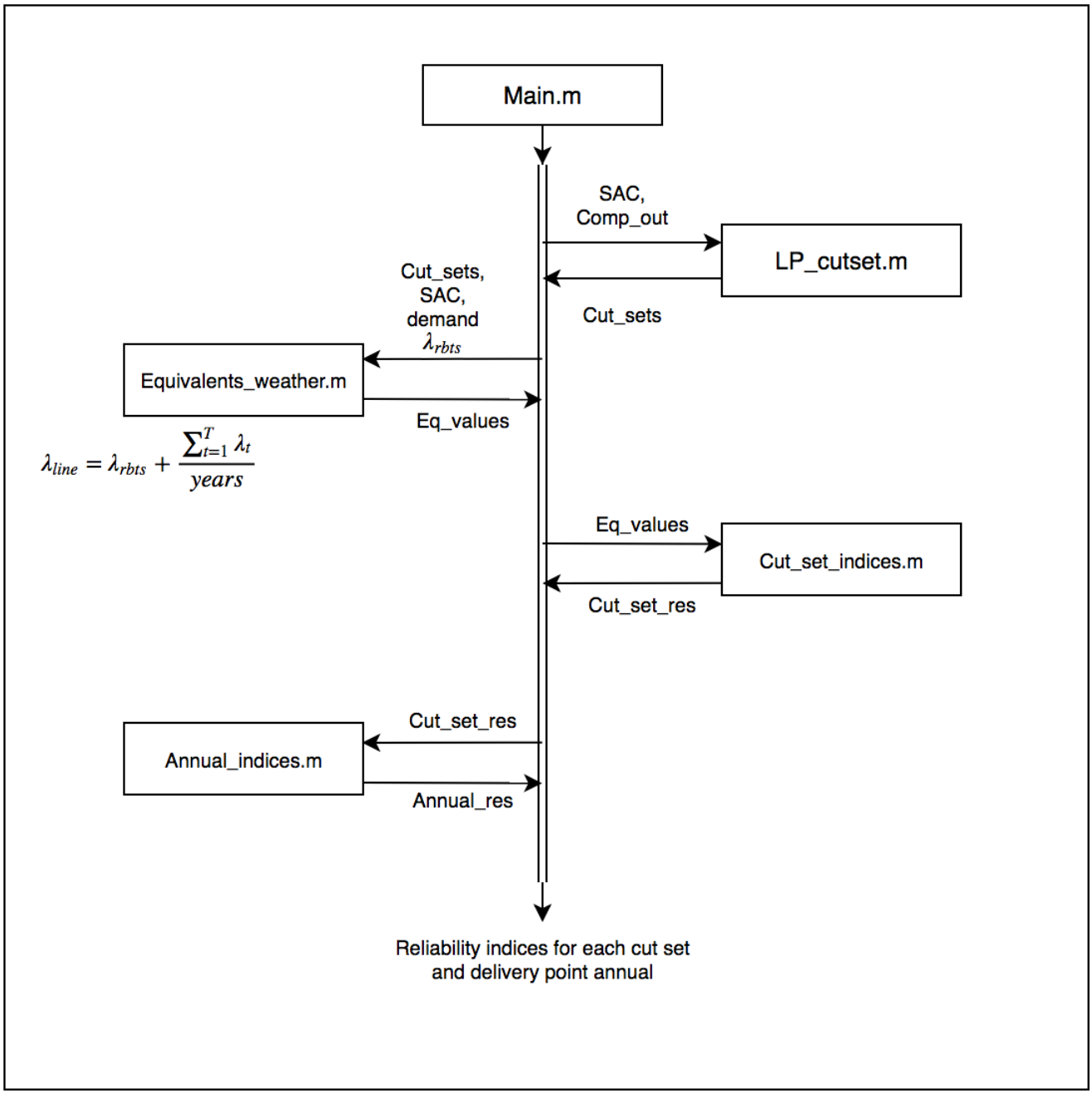

Figure 24: Code structure for the implementation of the OPAL Methodology and average weather. Arrows indicate control flow.

In the script `cut_set_indices.m` the ENS is calculated for each cut set using Equation (20). The annual interrupted power for every cut set is also calculated. These indices are then used in the script `annual_indices.m` where the annual delivery point indices are calculated by summing cut set indices related to the delivery point as described in Section 2.7.4. Indices for every cut set and load point is lastly returned as output in the form of a struct and as a table.

3.6.2 The Approximate Method

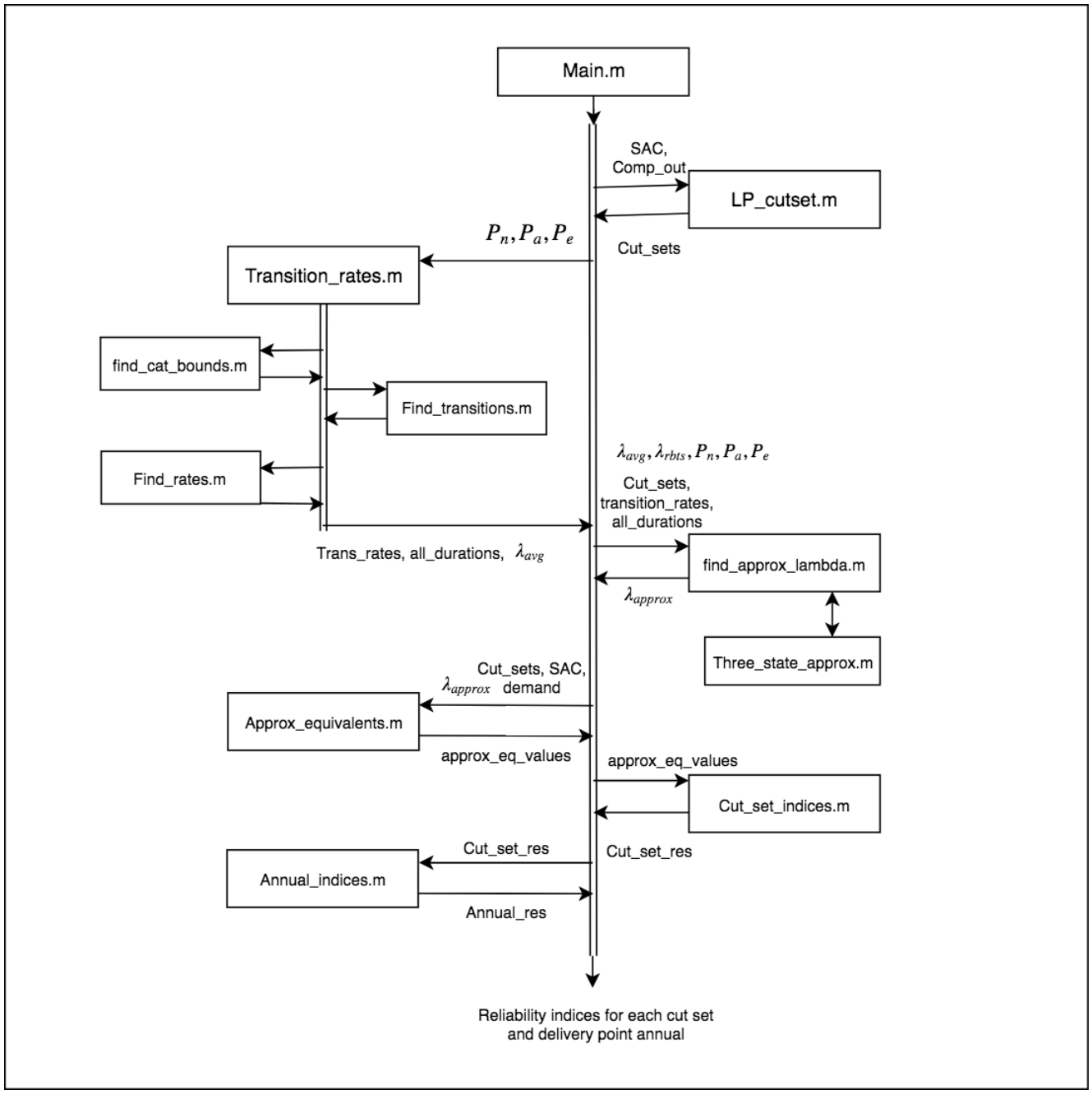

Figure 25: Code structure for the implementation of the approximate equations method

The code structure of the approximate equations method implementation is shown in Figure 25. main.m is the same as described above and defines all necessary input variables. The probabilities of residing in each weather state is defined here. To activate the approximate method, the parameter "approx" must be set to 1.

The script `LP_cutset.m` finds the minimal cut sets of the system as earlier described. However more input is needed to calculate the equivalent parameters of the cut sets following this method. These are calculated in the script `transition_rates.m`. This script calculates transition rates, duration matrix and the average failure rate for each weather state of each line. `transition_rates.m` has three sub-scripts conducting different tasks. `find_cat_bounds.m` finds the boundary values between the weather states in the time-series. This is done by sorting the probability of failure in increasing order, and applying the given probabilities of weather states. This is illustrated in Figure 23. It then sorts every hour of the time-series to the correct state and calculates λ_n, λ_a and λ_e for every line. The normal weather state in the code is denoted 1, adverse 2 and extreme is numbered 3.

The bounds of each category, which is unique for every line, is then used in `find_transitions.m` to register every transition that occur between each weather state and the duration of time within each state before the transition is made. This is registered in a duration matrix for each line with the format as illustrated in Table 13. Each placements in the matrix is an array of the number of hours the weather resided in the "from" state before the transition. `find_rates.m` then calculates the transition rates based on the duration matrix as described in Section 3.4.

The script `find_approx_lambda.m` calculates the equivalent failure rate of every minimal cut set. If the minimal cut set only contain one component the equivalent value is calculated as the λ_{rbts} added to the average wind-dependent failure rate from the time series. This is the same calculation as used for the average method. If the minimal cut set contain two components the equivalent failure rate is calculated using the approximate equations method implemented in the script `three_state_approx.m`. Here the base failure rate λ_{rbts} is added to the wind-dependent failure rates λ_n, λ_a and λ_e for each line. The average duration of weather states for each minimal cut set is calculated using the duration matrix of the two components. The minimal cut set transition rates are found by taking the average of the transition rates of the lines included in the set. λ_{approx} is then calculated using the scenario equations from Section 2.10.2.

Next `approx_equivalents.m` calculates the remaining equivalent values for each minimal cut set. This is P_{interr}, r_{eq} and U_{eq}. All equivalent values are then transferred to `cut_set_indices.m` to calculate cut set indices as earlier described. These are then used to calculate delivery point indices in `annual_indices.m`.

3.6.3 The Timestep Method

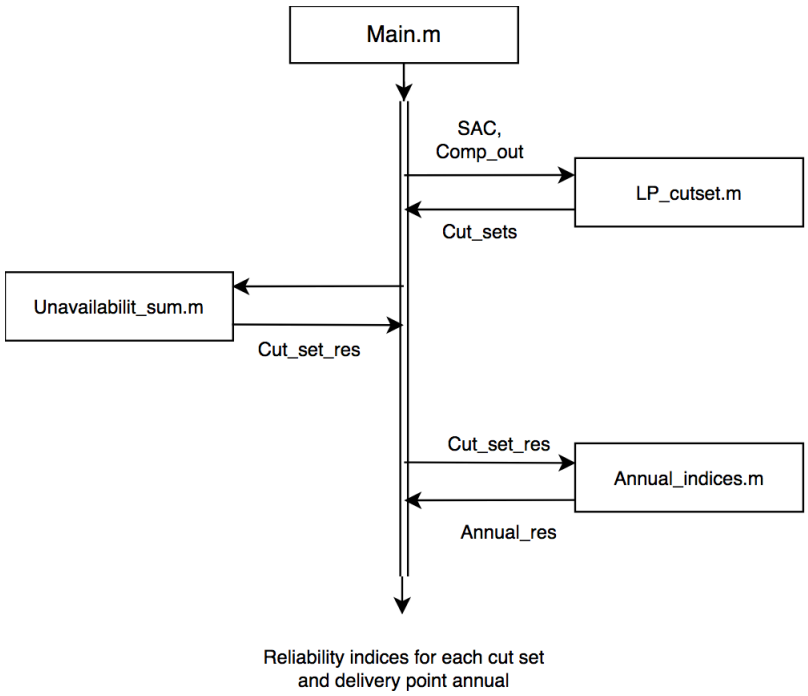

Figure 26: Code structure for the implementation of the timestep method

Here the code structure of the timestep method, utilizing the sum-equation from Equation (60), is shown. The code structure utilizing the more complex product-function from Equation (59) has the exact same code structure. The only difference is the calculation of the equivalent unavailability. The script run to use the product-function is called `unavailability_prod.m` and can be chosen from `main.m`. All scripts can be found in the Appendix.

The timestep method utilizes the same `main.m`, `LP_cutset.m` and `annual_indices.m` as earlier

described. The remaining actions are conducted by `unavailability_sum.m`. It loops through every hour of the time-series, adds λ_{rbts} to the weather dependent failure probability and calculates the unavailability of the minimal cut set at every hour as described in Equation (55) and (56). The average unavailability value, U_{eq}, for every cut set is then calculated as in Equation (57). In the same script the equivalent repair time, failure rate, interrupted power and ENS is calculated.

4 Results

4.1 Line Results

The resultant wind dependent failure rates from the time series are shown in Table 14. It contain the average failure rate of the time series, and the failure rates of each weather state when applying the three state weather model. It can be seen that line 3 has the highest wind impact, by a significant margin. Line 8 and 6 has the lowest weather impact with line 8 having the smallest average, but higher extreme impact than line 6.

	Average	N	A	E
Line 1	0.1182	0.08	3.5	17.3
Line 2	0.2292	0.15	7.8	40.3
Line 3	1.1345	0.84	28.2	145.8
Line 4	0.3747	0.26	11.4	52.3
Line 5	0.2490	0.15	9.3	50.5
Line 6	0.0167	0.01	0.6	3.6
Line 7	0.1225	0.08	3.9	17.0
Line 8	0.0128	0.006	0.6	4.9
Line 9	0.1206	0.08	4.0	17.9

Table 14: Line weather related failure rates $[\frac{1}{year}]$

4.2 Timestep Method

The timestep method has two possible calculation approaches. The sum method and the product method. The results for both methods are shown in Table 15. It can be seen that the results are equal until the third or fourth decimal of ENS for the second order minimal cut sets and after 2 decimals for cut set 9. This difference is considered neglectable, which shows that the simplification made in the sum method is viable. In the remainder of the thesis the Timestep method is represented by using the sum of the failure probabilities as in Equation (60). The sum method is chosen because it is less computationally demanding.

		Sum method	Product method
Delivery Point	Cut set	ENS	ENS
DP 2	6,7	1.99013282	1.99005696
DP 2	2,6	2.03640827	2.03616983
DP 2	1,7	2.15046542	2.15012693
DP 2	1,6	0.84895923	0.84888364
DP 2	1,2	2.22338230	2.22261063
DP 4	5,8	0.39500584	0.39464729
DP 5	9	255.94807982	255.92216303
DP 5	5,8	0.39500584	0.39464729

Table 15: Timestep method results

4.3 Failure Bunching

Figure 27 shows the ENS per year for the total system from each method. Here the interrupted power from every minimal cut set is included. The bar from the figure called Base shows the ENS, in blue, when no weather impact is included. This base is the result of the general RBTS input parameters, and is equal for every method studied. The red section of the bar chart depicts the impact of the weather dependent ENS. This varies from method to method, however it can be seen that the difference between methods including weather are small. The Base bar has a resultant ENS of 237.38 MWh/year. The Average bar represents ENS for the average method, which is described in Section 3.6.1. Remaining bars represents the other studied methods as labeled. It can be seen that the effect of including wind impact in reliability analysis is large, and increases total ENS with approximately 28 MWh each year which is significant.

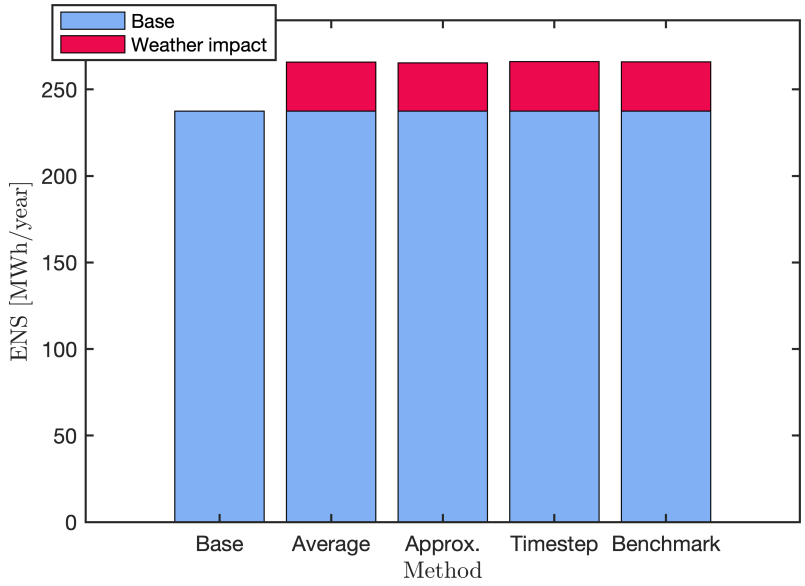

Figure 27: Total system ENS

To better see the difference between the methods including wind impact, Figure 28 shows the same data as Figure 27 focusing on the deviations. The black line indicates ENS for the benchmark indices. It can be seen that there is little difference in the resultant ENS of the four methods studied. The timestep method is furthest from the benchmark results with a difference of 0.15 MWh per year, however this is a relative difference of only 0.06% when comparing the total ENS with the benchmark results as the reference. The average method and approximate equations method are very close to the benchmark results, with a difference of 0.07 MWh and 0.03 MWh respectively, which can be considered neglectable. This shows that when studying the system as a whole, with the magnitude of weather impact from the input data-series, all methods calculate ENS within a reasonable error margin.

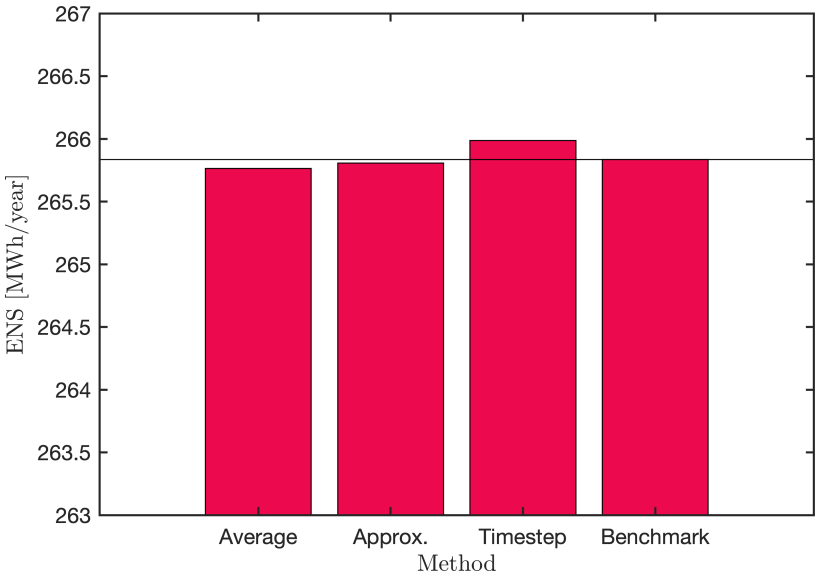

Figure 28: Total system ENS with weather impact included

The ENS for each delivery point is distributed as shown in Table 16. It can be seen that delivery point 1 and 3 never experience any interruption. DP 4 has the lowest ENS of the interrupted delivery points. DP 2 has a large yearly interruption and DP 5 has the significantly largest ENS. This distribution of interruption is consistent with the priority order interruption cost policy implemented and the system topology. DP 1 is the highest prioritized delivery point and is therefore never interrupted. DP 4 is the second highest prioritized, however if the minimal cut set 5,8 occur, DP 4 is separated from the system and is interrupted. The probability of this second order minimal cut set to occur is low, resulting in a low ENS of DP 4. Next, DP 3 is prioritized and never interrupted due to several alternative supply options. DP 5 is the fourth highest prioritized delivery point, however this delivery point is the only one not being N-1 secure. This results in an interruption if line 9 experiences a contingency. This is expected to occur once per year, which results in a high, unavoidable ENS. DP 2 has the second largest ENS due to the fact that it is the delivery point with the lowest IC. Whenever the system cannot supply the total demand of the system, delivery point 2 is cut due to the objective function of the OPF. It can also be seen that cut set 1,6 has a higher P_{interr} than the other cut sets at DP 2. This is because of the transfer capacity of line 1 and 6.

Delivery Point	Base	Average	Approx	Timestep	Benchmark
DP 1	-	-	-	-	-
DP 2	8.36640846	9.05405826	9.09984451	9.24934803	9.165171938
DP 3	-	-	-	-	-
DP 4	0.29702668	0.37563399	0.37385642	0.39500584	0.381929969
DP 5	228.71499064	256.33443007	256.33265249	256.34308567	256.2879098

Table 16: ENS at every delivery point [MWh/year]

The delivery point ENS is also given for each method studied. It can be seen that every method follows approximately the same magnitude and correlation of the delivery point. The base case without wind included is overall lower than the other methods, which show the importance of including weather. The effect of the methods on ENS will be exemplified by the minimal cut sets.

Every delivery point has ENS caused by minimal cut sets. These cut sets, and their corresponding DP, are shown in Table 17, with the interrupted power (P_{interr}) for each occurrence of the minimal cut. Detailed results of ENS, repair time and equivalent failure rate for every minimal cut set can be found in the Appendix. It can be seen from Figure 17 that DP 2 has the largest number of minimal cut sets. This is, as mentioned, due to this delivery point being interrupted whenever there is a general shortage of power in the system. This is due to the objective function of the OPF to minimize interruption cost.

Delivery Point	Cut Set	P_{interr}[MW]
DP 2	6,7	17,1552
DP 2	2,6	17,1552
DP 2	1,7	17,1552
DP 2	1,6	23
DP 2	1,2	17,1552
DP 4	5,8	20
DP 5	9	20
DP 5	5,8	20

Table 17: Minimal cut sets and interrupted power

4.3.1 First Order Minimal Cut Set

There is one first order minimal cut set in the system as seen in Table 17. This is a contingency on line 9 causing 20 MW of interrupted power on DP 5. The resultant ENS for each method is shown in Figure 29. Here the average and approximate method has the exact same ENS. This is due to the fact that the exact same method is used for both cases. The approximate method is only presented for second order cut sets. Therefore it has been chosen to calculate the first order cut set of the approximate equations method by utilizing the average method.

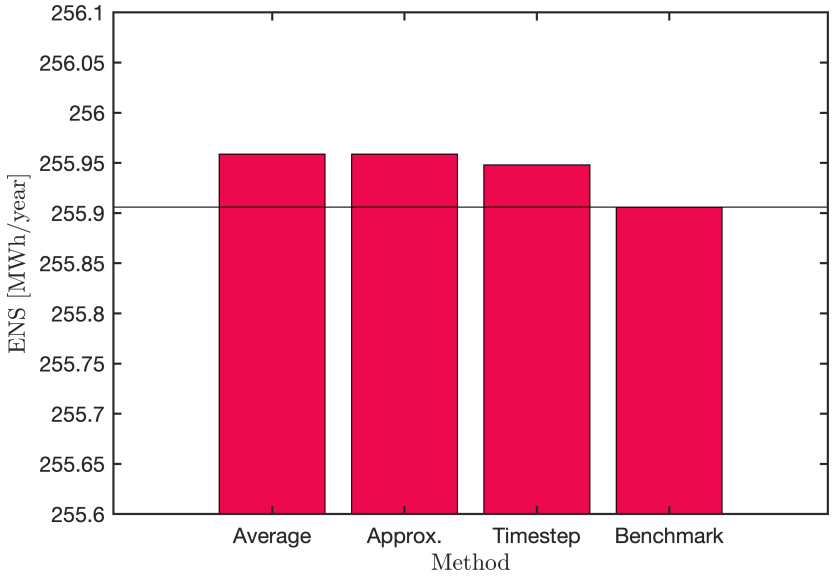

Figure 29: Cut set 9 ENS

The black line represents the ENS from the benchmark method as reference. It can be seen that all methods overestimate the ENS compared to the benchmark. The average method is slightly higher than the timestep method. The difference in the average method and the benchmark method is only approximately 0.05 MWh/year which is an neglectable difference with a total ENS of 255.96 MWh/year for the average method.

4.3.2 Second Order Minimal Cut Sets

There are several second order minimal cut sets in the system. In this section three cut sets are chosen for further analysis of results. These are cut set 6,7 1,2 and 5,8. Every cut set has unique characteristics which make them interesting to study closer. Cut set 6,7 and 1,2 has the exact same RBTS base situation, however cut set 1,2 experiences a large impact from wind-related failures and 6,7 has a small impact from wind-related failures. Cut set 5,8 is chosen because it has a small base ENS, but large weather impact. Results for all remaining cut sets can be found in the appendix.

Two aspects will be studied in this section; the ability of the method to capture failure bunching, and the calculation of ENS compared to the benchmark results. When studying the methods ability to capture failure bunching, the approximate, timestep and benchmark results will be compared to the standard calculation of indices including average wind impact wich is the method described in Section 3.6.1. This shows how the method captures wind-related failure bunching compared to the average method. The average method is chosen as reference because it is the easiest possible, and least computationally extensive method to include weather-related failure rate. The scope of this thesis includes the objective of recreating the benchmark results in a simplified method. Therefore the results from the average, approximate and timestep methods are shown for the cut sets compared to the benchmark data.

The plots indicate the deviation of the methods studied to the reference case. The black line in each plot indicates the reference value. Every bar is depicting a percentage for each method. This percentage is the relative deviation of the method compared to the reference method from the plot. Here it is important to highlight that the calculated percentage deviation is for the ENS caused by wind-related contingencies only. Every method has a base ENS caused by the general input parameters of the RBTS system. This ENS is equal independent of method chosen to implement failures caused by weather impact. If the percentage deviation was calculated including the RBTS base, the deviation would be misleadingly small.

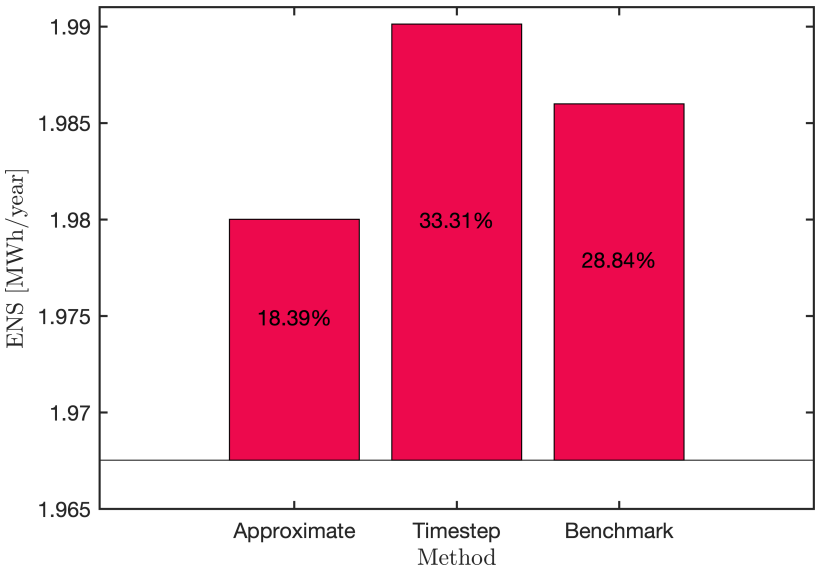

Figure 30: Cut set 6,7 compared to average weather

Figure 30 shows how the methods of cut set 6,7 capture failure bunching with the average method as reference. The black line shows the resultant ENS of the reference. It can be seen that all three methods capture significantly more wind-related ENS than the average method. Especially the timestep and benchmark method, with a relative deviation of 33% and 29% respectively, are able to improve the capture of failure bunching.

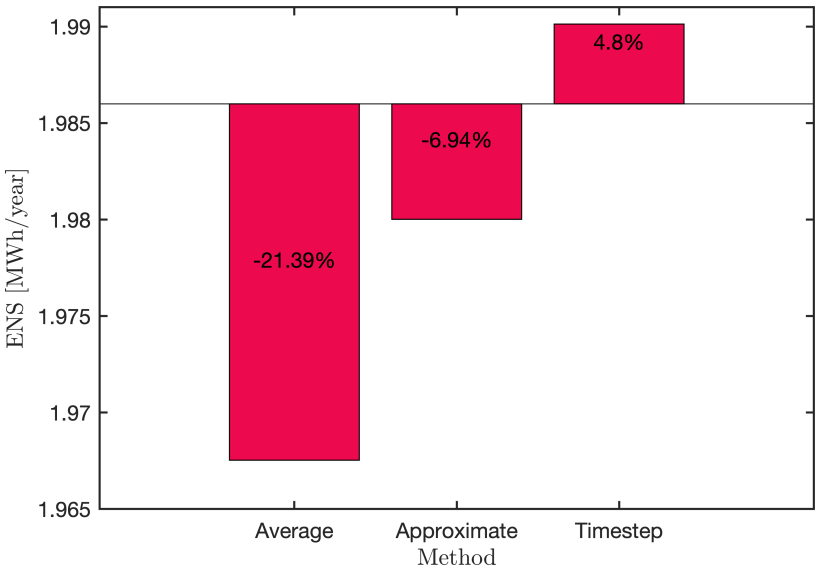

Figure 31: Cut set 6,7 compared to Benchmark

Figure 31 shows the same cut set 6,7 with the benchmark as the black line reference. It can be seen that the average method is furthest from recreating the benchmark results with a negative relative deviation of 21%. The timestep method is closest to benchmark results for cut set 6,7 with an overestimation of 5%. The approximate equations method has an underestimation of -7%. This is significantly better than the average method, however if the ENS of the cut set is large this may cause a prominent deviation of ENS.

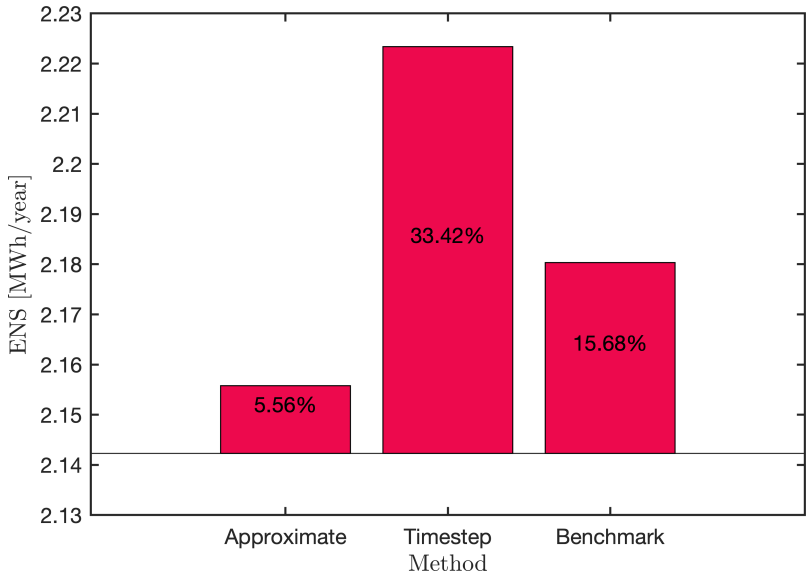

Figure 32: Cut set 1,2 compared to average weather

Figure 32 shows how failure bunching is captured for each method when applied to cut set 1,2. All methods capture more wind-related ENS than the average method. The approximate method captures almost 6% more, which is the smallest deviation from the average method. This results in a deviation of 0.014 MWh/year. The largest deviation is for the timestep method with more than 33% relative deviation. The benchmark method resides in between, with almost 16%. Except for the timestep method, the more complex methods has a smaller deviation in capturing failure bunching when weather impact increases when compared to the average method

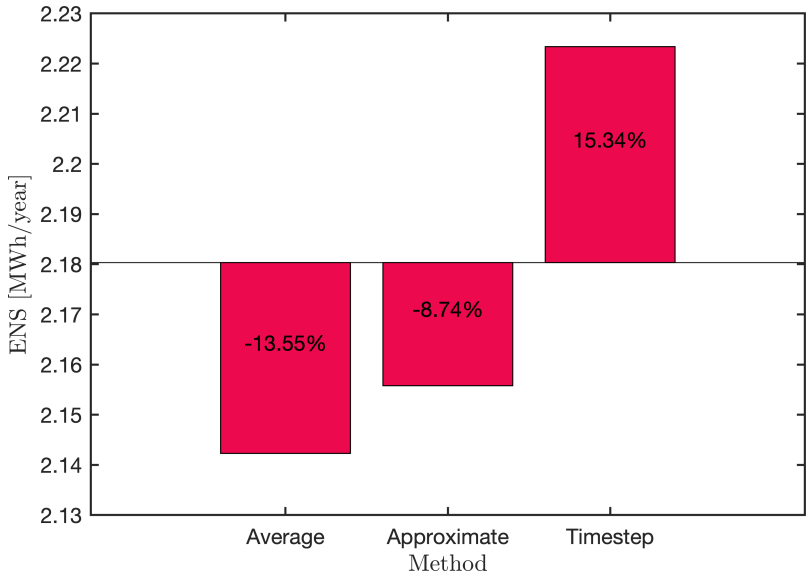

Figure 33: Cut set 1,2 compared to benchmark

Figure 33 shows the weather-related ENS compared to the benchmark results. It can be seen that the approximate method is closest benchmark with an underestimation of almost 9%. This is a slightly higher deviation than for cut set 6,7, but the deviation remains stable. The average method is significantly closer to the benchmark method when the wind-impact of the lines in the cut set increases. The timestep method deviation to benchmark is significantly increased, now with a deviation of 15%. This shows that the accuracy of the timestep method worsens as the ratio of wind-related failures increase.

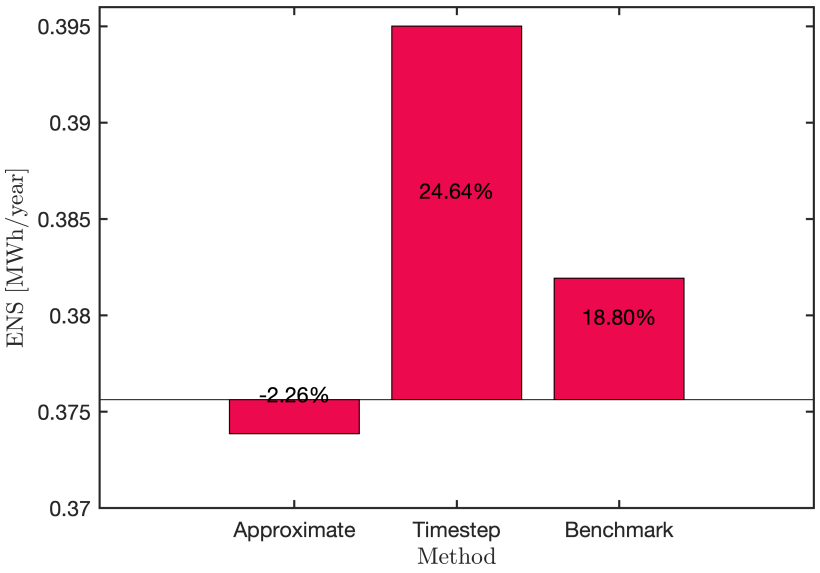

Figure 34: Cut set 5,8 compared to average weather

Cut set 5,8 can not directly be compared to cut set 1,2 and 6,7. This is because it has a different RBTS base case and are affecting an other delivery point. The cut set is still interesting to study due to its high priority in the system and low probability of occurrence. It also has highly weather impacted lines as seen in Table 14 and a small RBTS failure rate. The methods ability to capture failure bunching is shown in Figure 34. It can be seen that the timestep method clearly captures the most wind-related ENS. The benchmark method has a relative increase of almost 19% wind-related ENS, which will constitute a large deviation if the weather impact is increased. It can be seen that the approximate method captures 2%less wind-related ENS than the average method. The reasons behind this will be discussed further.

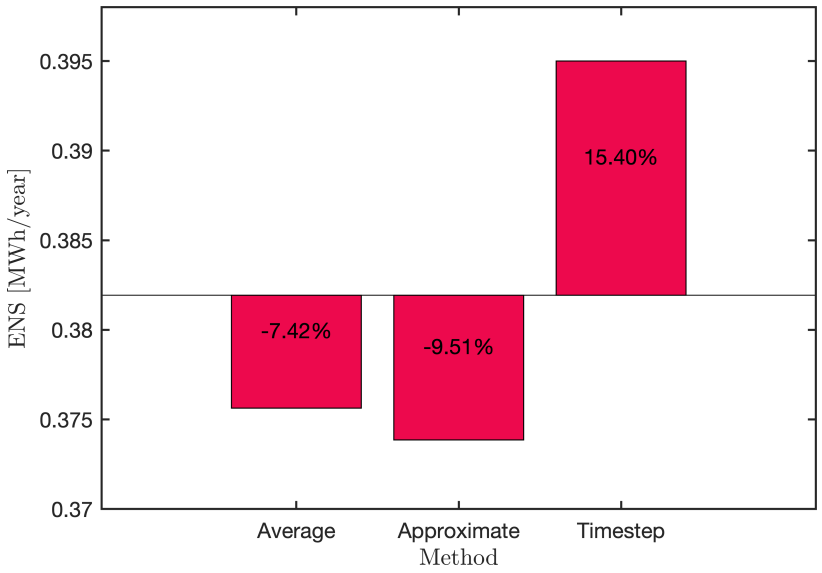

Figure 35: Cut set 5,8 compared to Benchmark

Figure 35 shows the results compared to the benchmark results. It can be seen that the average method actually has the best fit with a 7% underestimation and 0.006 MWh difference. Here the timestep method again overestimates and the approximate method underestimates with 9.5%. This is consistent with the magnitude of the deviation of previously discussed cut sets.

4.4 Approximate Equations Method

In this sections the contribution to λ_{approx} from each weather category and scenario in the approximate equations method will be discussed. The same minimal cut sets as above will be studied. This is conducted to further understand the approximate equations method, and see which scenarios contributes to the equivalent failure rate and ENS. It will also give an indication of which weather scenario which may be neglected to reduce computational time.

Table 18 shows the contribution to λ_{approx} for cut set 6,7. These are shown in actual value and in percentage of total λ_{approx}. It can clearly be seen that the scenario NN, where both failures occur in normal weather, is the largest contributor with almost 98%. The NA scenario is also a large contributor due to the large occurrence of the transition from normal to adverse weather, and

the large probability of initially residing in the normal category. The AA and EE scenarios, where both contingencies occur in adverse and extreme weather respectively, contribute to the resultant λ_{approx}, however not by a large percentage due to the small weather impact on this minimal cut set. The scenarios NE, AN, AE, EN and EA has neglectable impact due to the small number of observed transitions, or the unlikeliness of weather states.

Scenarios	λ_{approx}	Percentage
NN	0.019771595	97.834 %
NA	2.98E-04	1.477 %
NE	6.69E-07	0.003 %
AN	6.69E-07	0.003 %
AA	1.32E-04	0.654 %
AE	3.57E-08	0.000 %
EN	7.71E-11	0.000 %
EA	4.06E-10	0.000 %
EE	5.66E-06	0.028 %
Total	0.0202	

Table 18: Cut set 6,7

Table 19 shows the contribution to equivalent failure rate for cut set 1,2 when applying the approximate equations method. As previously mentioned, this cut set has the exact same base situation as cut set 6,7, but with larger weather impact of lines. It can be seen that this is reflected in the equivalent equations results due to the increased percentage of contribution from adverse and extreme categories. In scenario NN, the impact from this state is higher than the impact from NN in cut set 6,7, even though the percentage of total λ_{approx} is smaller. This is due to the increased failure rate of normal weather as shown in Table 14. In this cut set the NA scenario has the second largest contribution to λ_{approx} with 2.6%. AA and EE has increased impact compared to cut set 6,7 and AA in particular has a significant increase and contribution to results. The scenarios NE and AN also has an increased impact compared to cut set 6,7 and with increased weather, these scenarios may have an notable impact on ENS. However they are still small compared to total equivalent failure rate. AE, EN and EA are still neglectable.

Scenarios	λ_{approx}	Percentage
NN	0.020971205	95.297 %
NA	5.71E-04	2.597 %
NE	2.64E-06	0.012 %
AN	5.87E-06	0.027 %
AA	4.15E-04	1.888 %
AE	1.53E-07	0.001 %
EN	3.03E-10	0.000 %
EA	1.74E-09	0.000 %
EE	3.95E-05	0.179 %
Total	0.0220	

Table 19: Cut set 1,2

Table 20 shows the resultant contributions to cut set 5,8 when applying the approximate equations method. As previously mentioned, this cut set has a small base ENS and failure rate from the RBTS system, but a large weather impact as shown in Table 14. This is confirmed in Table 20. It can be seen that λ_{approx} is small due to the small RBTS failure rate, however the percentage in NN is significantly smaller than in previous cut sets. This is highly influenced by the small constant failure rate of the base RBTS input values in combination with the high wind-impact of the lines. This is because the wind-related failure rate constitutes a larger portion of the total failure rate. E.g. a wind-related failure rate of 4 has a larger relative impact on the system if the RBTS base-failure rate is 1 in the case of lines 5 and 8 than for line 2 with the RBTS-base failure rate of 5.

With a small base failure rate, the large weather dependent λ will be more prominent and have a relative larger impact. It can be seen that the NA and AA scenarios are almost doubled in percentage, while the EE scenario constitutes 0.39% which is more than double of the cut set from 1,2. The results of cut set 5,8 mirror the pattern of cut set 1,2, where both have large weather impact, with a small contribution from NE and AN and with neglectable impact from AE, EN and EA.

Scenarios	λ_{approx}	Percentage
NN	0.00298841	91.293 %
NA	1.52E-04	4.636 %
NE	1.66E-06	0.051 %
AN	1.56E-06	0.048 %
AA	1.17E-04	3.583 %
AE	5.21E-08	0.002 %
EN	1.28E-10	0.000 %
EA	6.14E-10	0.000.%
EE	1.27E-05	0.389 %
Total	0.0033	

Table 20: Cut set 5,8

Computing the results of the approximate equations method for a three state system is more computational extensive than for a two state system. The two state system will consist of 5 scenarios compared to the 9 scenarios of the three state system. Extra computations of transition rates, failure rates and durations are also necessary. As seen in Table 18-20, the only contribution from the extreme category is scenario EE, where both contingencies occur in the extreme weather state. Therefore it can be debated if the extreme weather state is necessary to include when using historic data.

5 Discussion and Comparison

The aim of this master thesis is to capture failure bunching in reliability analysis of power systems due to increased weather impact, by including wind-related failures. It can clearly be seen from Figure 27 that the inclusion of wind related failures increases the total ENS of approximately 28 MWh/year. This is a significant increase which is important to include in power system planning methodologies to optimize mitigation.

The results when analyzing the ENS of the system as a whole shows that all methods studied are within an acceptable error margin and can be used. However, is only certain for the case with the input data-series studied for the RBTS system and not as a general fact. If the weather impact of the input data is increased, the characteristics of each method, as studied for each cut set, will become more prominent. The input data-series used in this thesis has approximately 10% of contingencies due to wind. As discussed in Section 2.8, the environmental impact on the system is much larger. If more wind-impact is included in the input data-series and more data is available for several environmental phenomena, the weather impact will increase, and the choice of weather implementation method is important.

5.1 Average Method

The average method is used as a reference, and is the easiest possible way of capturing weather impact. It gives a decent representation, however it does not capture failure bunching as well as the other methods. When studying cut set 6,7 and 1,2 which has the same base, it can be seen that the average method has a decreasing percentage error when weather impact increases. In the cut set 5,8, which has large weather impact, but small RBTS base, the average method is the most accurate. The average method has proven to be more accurate than initially expected, however it is unstable in deviation to the RBTS method, and captures less weather-related ENS than other methods in general. The reason is because the method does not differentiate between a large storm or a day with no wind. A lot of information and detail is lost when only including the average of the time-series of each line.

5.2 The Approximate Equations Method

The approximate equations method captures failure bunching better than the average method. This is because it includes weather states which are able to capture more variances in the time-series input data, and less information is lost. It is also the method which is closest to the benchmark results for the system as a whole as seen in Figure 28. It consistently underestimates results when compared to benchmark, and the deviation is consistent whether lines in the cut set has a large or small probability of failure.

The approximate equations method has a consistent contribution to λ_{approx} from the scenarios for all minimal cut sets. The NN scenario has the largest contribution due to the long duration of normal weather and large probability of initially residing in this state. The NA scenario has the second largest contribution to λ_{approx} due to the high probability of the transition from normal to adverse state, and the high probability of the first contingency to occur in the normal state.

It is interesting to study the relationship between the probability of residing in the weather state of the initial contingency, and the probability of transfer between states. The NA scenario is the second largest with both high probability of residing in the initial state, and a high probability of transition. With AN, the probability of transition is high and with NE the probability of residing in the initial state is high, but the probability of transition is very low. E.g the probability of residing in each weather state initially is given by Table 12. For line 1, the expected number of transitions for AN is almost 30 transitions per year, for comparison, the transition rate of NA is equal. For NE only one transition is recorded for the whole period of 25 years resulting in a transition rate of 0.04 per year. For cut set 6,7 the contribution to λ_{approx} is equal. In cut set 1,2, AN has a higher contribution than NE, while for cut set 5,8 NE is slightly higher. The ratio between the probabilities of initially residing in normal or adverse weather states are approximately 1%. The ratio between the transition rates for AN and NE for line 1 is 0.01%. Still the results of the two scenarios are very similar, which shows that the probability of residing in the initial state of the first contingency is more important for results than the probability of transition between states. Here it should be noted that the relationship between transition rates are very similar for each line.

The scenarios EN and EA has very few expected transitions during a year, and the extreme weather state has a low probability of initially occurring. Therefore these scenarios can easily be neglected to reduce computational time.

All scenarios containing the extreme weather state does not affect ENS much. In the cut set 5,8, which has the largest contribution outside NN, the total contribution from scenarios containing failure in the extreme state is 0.442% which is very small. Including the extreme weather state in the method entails increased computational time in every step. The sorting of the time-series requires an additional possible state, transition rates are increased from 4 to 9 and so is the number of scenarios calculated. [1] shows an significant increase in ENS when the extreme category is included. In the article, the input data are based on a fictional case with an assumed reality, and this may not be correct and over estimate the importance of the extreme category.

[1] calculated the λ_{approx} for different cases containing an increasing percentages of failures occurring in bad weather. By reproducing the approach in Section 3.3 it was possible to find the failure rates for each case as shown in Table 10. From this table the case where 10% of failures occur in bad weather is coherent with the historic time-series data used in this thesis. It should be noted that the input data and method of calculating the failure rates in the paper and in this thesis are not equal, and these failure rates can not be directly compared to calculated line failure rates in Table 14. However, it is possible to see some similarities in the scale of the values. Billinton often uses an error factor in his work[2][7]. This error factor is the ratio of increase in the failure rate when including failure bunching compared to it not being included [1]. For the 10% bad weather case in the paper, the error factor is 1.27, as a reference no change in failure rate has an error factor of 1. This indicates an increase in failure rate of 27%. The same paper presents the error factor when only two states are used, and with the two state model, the error factor is also 1.27 for the case with 10% weather impact. This indicates that there is no difference in the two and three state model with a small percentage of failures occurring in bad weather. As discussed in Section 2.8, the historic wind impact on the Norwegian power grid is approximately twenty percent. In the Billinton paper, when 20% of failures occur in "bad weather", the error factor for the three state system is 2.06. For the two-state model the same case has an error factor of 2.04, which is a 2% deviation when the extreme weather state is included. With increasing number of failures occurring in the extreme weather case, the error factor is also increasing. It is natural to assume this is also the case with the use of the approximate equations method on historic data.

When developing methodologies for reliability analysis of power systems, there is always a balance between computational time and accuracy of results. With the time-series input of historic wind data used in this thesis, which accounts for approximately 10% of contingencies occurring due

to wind, a two state method should suffice. However, with increasing number of environmentally related contingencies and extraordinary weather phenomena the three state weather model is most likely necessary to capture failure bunching because the contribution from the extreme categories are increasing with weather impact. This should be further studied by testing the method on data with increased ratio of weather-related failures.

5.3 The Timestep Method

The timestep method consistently overestimates the resultant ENS for every cut set. The overestimation also increases when the weather impact of the lines in the cut set increase. With the increase of weather related contingencies, the error and overestimation will become larger, making this method unsuitable. This method is also the one furthest from the benchmark for the overall system. The capture of failure bunching is larger, however it is not desirable to capture failure bunching effects that are non-existent in the real system.

The timestep method is a simplified implementation of the benchmark method, where the difference is the consideration of the outage duration. In the benchmark method the outage duration is found through a survival function which is based on probabilistic methods and historic data as described in Section 3.1.1. The timestep method assumes a constant outage duration for all cut sets which are chosen as the average of the benchmark survival function. The oscillations of the unavailability in the time-series are amplified compared to the benchmark method. This can be seen for line 9 in Figure 38 in the Appendix. All lines follow this pattern. When the unavailability of the line has a peak, the peak of the timestep method is elevated compared to the benchmark method. This is also the case for the dips in the unavailability. When the unavailability drops, the timestep method gets a lower unavailability than the benchmark method. Because the peaks result in a higher unavailability and deviation to the benchmark results, the equivalent unavailability of the line overestimates compared to the benchmark result. This again results in an overestimated ENS. This also explains why the overestimation increases with increased wind impact.

5.4 Comparison of Methods

All methods can be used on the RBTS system with results within an acceptable margin of error. However, the methods do have significant relative deviations when studying the minimal cut sets.

With the input data and system studied in this thesis, the absolute deviation in MWh/year for the methods has been small. This is somewhat due to the large ENS caused by the base RBTS system indices. When only studying the contribution from the weather-related indices, the relative deviation is larger. If the weather-impact of the input data increases, these deviations will result in notable changes in ENS for the system as a whole too.

The average method has proven to be more accurate than previously envisioned, especially when the weather impact was increased. However, the deviation to the benchmark method is non-consistent. Data is lost in the process, and it is unsuitable to capture and distinguish HILP events.

The timestep method consistently overestimates the ENS of each minimal cut set, and the system as a whole. The fact that the deviation to benchmark results increase with increased weather makes the method unsuitable. The timestep method was constructed based on the benchmark method, with constant outage duration. This shows the importance of how the outage duration is included in analysis.

The approximate equations method underestimates the ENS compared to the benchmark method. This under estimation is stable between 7-9% deviation. The deviation of the total system is less than 1%. For some cut sets other methods are closer than the approximate equations method, however this method is consistent. It looses less data than the average method due to utilizing weather states. It also has the ability to capture HILP events through the extreme weather state. It also has the ability to study which weather states and scenarios that contribute to λ_{approx}. Scenarios and weather states can also be reduced to further reduce computational time based on the scope of analysis and the weather impact of the input data.

6 Conclusion

In this thesis two methods of implementing weather data in reliability analysis has been developed and studied. This is the three state approximate equations method, which is altered to fit historic weather data as input, and the timestep method. These are tested and compared to standard reliability methodologies, a method including average weather impact and a more complex benchmark method.

An implementation in MATLAB based on the OPAL prototype has been developed for each method and tested. Results have been studied to find the most suitable approach. This has been based on two criteria, the methods ability to capture failure bunching and its ability to recreate results from the benchmark method with reduced computational complexity.

The approximate equations method has proved to be implementable on historic weather data with some changes, and is recommended as the most suitable approach. It captures more failure bunching than the average approach. The deviation to the benchmark method is the overall closest with a difference of 0.15 MWh/year. Out of a total ENS of 265.84 MWh/year this deviation is minimal. On minimal cut set level, the deviation when only considering weather-related ENS is 7-9% when compared to the benchmark method. This is a absolute deviation of 0.025 MWh/year for cut set 1,2 which has the largest deviation. This magnitude is considered neglectable.

With the input data-series used in this thesis for the RBTS system the extreme category is not highly affecting results, and the two state method can be used. This is because the input data series has 10% of failures occurring due to wind. With several weather phenomena included in the input data series with a higher overall percentage of weather-related failures, the extreme weather category may be more prominent. The extreme category may be suitable to capture HILP events, however more studies on the method with input data containing higher degree of weather-impact is necessary. Some scenarios can be removed to ease computational time and complexity further.

The timestep method consistently overestimates ENS and is the furthest from benchmark results. It captures more failure bunching than the approximate method, however capturing non-existent weather impact is not desirable. The overestimation increases with increasing weather impact, which makes this method unsuitable.

6.1 Further Work

Several observations has been done through working with this thesis that has been outside the scope. One is the importance of outage duration or repair time. The major difference between the timestep method and the benchmark method is the handling of the outage duration. The importance of the assumption that repair is only conducted in the normal weather state in the approximate equations method is also interesting to study further.

Most parameters are based on the input time-series of the hourly failure probabilities. However, the probability of residing in each weather state is taken from literature. It is important to study the affects of this probability which is not based on the historic weather data. This can be conducted through a sensitivity analysis. It is also interesting to optimize the categorizing the input time-series in weather states.

The methods have only been tested on one set of input data. Further testing with other input data sets are necessary. Especially more information about the necessity of the extreme weather state in the approximate equations method when the ratio of weather related failures is increased is interesting to study further.

The duration matrix used to find the average duration and transition rates of the system and weather states was observed to be very symmetric. This is interesting to study further. There is also potential in utilizing the conditional probability table(CPT) in a model based on Bayesian networks. Where observed transitions from the duration matrix can be used as the basis of the CPT.

References

[1] R. Billinton, C. Wu, and G. Singh. Extreme adverse weather modeling in transmission and distribution system reliability evaluation. Jan 2002.

[2] R. Billinton and R.N. Allan. *Reliability Evaluation of Power Systems*. 1996.

[3] G.H Kjølle and O. Gjerde. "The OPAL methodology for reliability analysis of power systems". *SINTEF Energy Research*, 2012.

[4] Statnett SF. Årsstatistikk 2016 - Driftsforstyrrelser og feil i 33-420 kV-nettet. pages 1–38, 2017.

[5] G. Kjølle, R. H. Kyte, H. Vefsnmo, and J. Lille-Mæhlum. Analyser av feil og avbrudd i kraftnettet 1989-2011. *SINTEF Energi. Rapport*, (TR A7279), 2013.

[6] R. Billinton and K. E. Bollinger. Transmission system reliability evaluation using markov processes. *IEEE Transactions on Power Apparatus and Systems*, PAS-87(2):538–547, Feb 1968.

[7] R. Billinton and G. Singh. Application of adverse and extreme adverse weather: modelling in transmission and distribution system reliability evaluation. *IEEE Proceedings - Generation, Transmission and Distribution*, 153(1):115–120, Jan 2006.

[8] R. Billinton, S. Kumar, N. Chowdhury, K. Chu, K. Debnath, L. Goel, E. Khan, P. Kos, G. Nourbakhsh, and J. Oteng-Adjei. A reliability test system for educational purposes-basic data. *IEEE Transactions on Power Systems*, 4(3):1238–1244, Aug 1989.

[9] P. Kundur, J. Paserba, V. Ajjarapu, G. Andersson, A. Bose, C. Canizares, N. Hatziargyriou, D. Hill, A. Stankovic, C. Taylor, T. Van Cutsem, and V. Vittal. Definition and classification of power system stability ieee/cigre joint task force on stability terms and definitions. *IEEE Transactions on Power Systems*, 19(3):1387–1401, Aug 2004.

[10] CORDIS. Generally accepted reliability principle with uncertainty modelling and through probabilistic risk assessment.

[11] S. Perkin, G. Bjornsson, I. Baldursdottir, M. Palsson, R. Kristjansson, H. Stefansson, P. Jensson, E. Karangelos, and L. Wehenkel. Framework for threat based failure rates in transmission

system operation. In *2016 Second International Symposium on Stochastic Models in Reliability Engineering, Life Science and Operations Management (SMRLO)*, pages 150–158, Feb 2016.

[12] S Perkin. *Real-time weather-dependent probabilistic reliability assessment of the Icelandic power system*. PhD dissertation, Reykjavik University, 2018.

[13] R Billinton and R.N Allan. *Reliability Evaluation of Engineering Systems: Concepts and Techniques*. Springer US, 2 edition, 1992.

[14] A.G. Jensen. Capturing weather related common cause contingencies in power system reliability analysis. Dec 2017.

[15] A. Helseth, G. Warland, and B. Mo. Long-term hydro-thermal scheduling including network constraints. In *2010 7th International Conference on the European Energy Market*, pages 1–6, June 2010.

[16] K. Samdal, G. H. Kjølle, O. Gjerde, J. Heggset, and A. T Holen. Requirement specification for reliability analysis in meshed power networks. *SINTEF Energy Research*, TR A6429, Dec 2006.

[17] R.D Zimmerman and C.E Murillo-Sanchez. Matpower 6.0 user's manual. *Power Systems Engineering Research Center*, Dec 2016.

[18] G. Kjølle, R.H. Kyte, M. Tapper, and K. Hänninen. Major Storms – Main Causes , Consequences and Crisis Management. *22 nd International Conference on Electricity Distribution*, (Paper No 0658), 2013.

[19] SINTEF Energy research. Vulnerability and security in a changing power system. `https://www.sintef.no/projectweb/vulnerability-and-security/` [Accessed 25. Oct 2017].

[20] R. Billinton. Basic models and methodologies for common mode and dependent transmission outage events. In *2012 IEEE Power and Energy Society General Meeting*, pages 1–7, July 2012.

[21] R. Billinton and J. Acharya. Distribution system reliability assessment incorporating weather effects. 1:282–286, Sept 2006.

[22] R. Billinton and J. Acharya. Consideration of multi-state weather models in reliability evaluation of transmission and distribution systems. In *Canadian Conference on Electrical and Computer Engineering, 2005.*, pages 916–922, May 2005.

[23] R. Billinton and Chenjian Wu. Predictive reliability assessment of distribution systems including extreme adverse weather. In *Canadian Conference on Electrical and Computer Engineering 2001. Conference Proceedings (Cat. No.01TH8555)*, volume 2, pages 719–724 vol.2, May 2001.

[24] Y. Liu and J. Zhong. Risk assessment of power systems under extreme weather conditions — a review. In *2017 IEEE Manchester PowerTech*, pages 1–6, June 2017.

[25] Ø.R. Solheim, L. Warland, and T. Trotscher. A holistic simulation tool for long-term probabilistic power system reliability analysis. 2018.

[26] T.R Solheim, T Trötscher, and G.H Kjølle. Wind dependent failure rates for overhead transmission lines using reanalysis data and a Bayesian updating scheme. page 6, 2016.

[27] M. Panteli and P. Mancarella. Influence of extreme weather and climate change on the resilience of power systems: Impacts and possible mitigation strategies. *Electric Power System Research*, 127:259–270, 2015.

[28] M. Panteli and P. Mancarella. Modeling and evaluating the resilience of critical electrical power infrastructure to extreme weather events. *IEEE Systems Journal*, 11(3):1733–1742, Sept 2017.

[29] M. Panteli, C. Pickering, S. Wilkinson, R. Dawson, and P. Mancarella. Power system resilience to extreme weather: Fragility modeling, probabilistic impact assessment, and adaptation measures. *IEEE Transactions on Power Systems*, 32(5):3747–3757, Sept 2017.

[30] I. B. Sperstad and E. S. Kiel. Development of a qualitative framework for analysing high-impact low-probability events in power systems. pages 1599–1607, 2018.

[31] Y. Zhou, A. Pahwa, and S. Yang. Modeling weather-related failures of overhead distribution lines. *IEEE Transactions on Power Systems*, 21(4):1683–1690, Nov 2006.

[32] K. Murray and K. R. W. Bell. Wind related faults on the gb transmission network. In *2014 International Conference on Probabilistic Methods Applied to Power Systems (PMAPS)*, pages 1–6, July 2014.

[33] D. P. Gaver, F. E. Montmeat, and A. D. Patton. Power system reliability i-measures of reliability and methods of calculation. *IEEE Transactions on Power Apparatus and Systems*, 83(7):727–737, July 1964.

[34] R. Billinton and M. S. Grover. Quantitative evaluation of permanent outages in distribution systems. *IEEE Transactions on Power Apparatus and Systems*, 94(3):733–741, May 1975.

[35] L. Du, Y. Hu, and W. Han. Transmission and distribution system reliability evaluation based on three-state weather model. pages 1–4, March 2011.

[36] E.S. Kiel and G. H. Kjølle. Transmission line unavailability due to correlated threat exposure. December 2018.

[37] Kjeller Vindteknikk. Long term data-series, wrf era-interim.

[38] G.H Kjølle, A.O Eggen, H.M Vefsmo, J. Heggset, A. Bostad, T Trøtscher, and Ø.R Solheim. Norwegian disturbance management system and database. *CIGRE*, 2016.

[39] W. Wangdee and R. Billinton. Impact of load shedding philosophies on bulk electric system reliability analysis using sequential monte carlo simulation. *Electric Power Components and Systems*, 34(3):355–368, 2006.

[40] I.B. Sperstad and S.H. Jakobsen. Documentation of the opal prototype. *SINTEF Energi AS*, Project no. 502001246, Nov 2018.

7 Appendix

7.1 All Results

7.1.1 ENS

DP	Min Cut Set	λ_{eq}	Annual ENS
Load 1	-	-	-
Load 2	6,7	0,01939200	1,89971251
Load 2	2,6	0,01939200	1,89971251
Load 2	1,7	0,01939200	1,89971251
Load 2	1,6	0,00584404	0,76755842
Load 2	1,2	0,01939200	1,89971251
Load 3	-	-	-
Load 4	5,8	0,00260073	0,29702668
Load 5	9	1,00000000	228,41796396
Load 5	5,8	0,00260073	0,29702668
Total			237,37842577

Table 21: All results for base case. No weather included

DP	Min Cut Set	λ_{eq}	Annual ENS
Load 1	-	-	-
Load 2	6,7	0,02008435	1,96753784
Load 2	2,6	0,02049964	2,00822185
Load 2	1,7	0,02142541	2,09891318
Load 2	1,6	0,00637330	0,83707164
Load 2	1,2	0,02186844	2,14231375
Load 3	-	-	-
Load 4	5,8	0,00328901	0,37563399
Load 5	9	1,12057209	255,95879608
Load 5	5,8	0,00328901	0,37563399
Total			265,76412233

Table 22: Results for the average method

DP	Min Cut Set	λ_{eq}	Annual ENS
Load 1	-	-	-
Load 2	6,7	0,02021165	1,98000844
Load 2	2,6	0,02058829	2,01690596
Load 2	1,7	0,02154045	2,11018275
Load 2	1,6	0,00637226	0,83693462
Load 2	1,2	0,02200623	2,15581274
Load 3	-	-	-
Load 4	5,8	0,00327344	0,37385642
Load 5	9	1,12057209	255,95879608
Load 5	5,8	0,00327344	0,37385642
Total			265,80635341

Table 23: Results for the approximate equations method

DP	Min Cut Set	λ_{eq}	Annual ENS
Load 1	-	-	-
Load 2	6,7	0,02027270	1,985992927
Load 2	2,6	0,02070657	2,028496372
Load 2	1,7	0,02171775	2,127555086
Load 2	1,6	0,00641680	0,842784466
Load 2	1,2	0,02225660	2,180343086
Load 3	-	-	-
Load 4	5,8	0,00334413	0,381929969
Load 5	9	1,12034087	255,9059798
Load 5	5,8	0,00334413	0,381929969
Total			265,83501172

Table 24: Results of the benchmark method

7.1.2 Deviations

	Approximate vs Average		Timestep sum vs Average		Timestep prod vs Average		Benchmark vs Average	
Cut sets:	Total	Weather only	Total	Weather only	Total	Weather Only	Total	Weather Only
6,7	0,6338 %	18,386 %	1,1484 %	33,313 %	1,1445 %	33,202 %	0,94 %	27,210 %
2,6	0,4324 %	8,003 %	1,4036 %	25,976 %	1,3917 %	25,756 %	1,01 %	18,685 %
1,7	0,5369 %	5,657 %	2,4561 %	25,880 %	2,4400 %	25,710 %	1,36 %	14,378 %
1,6	-0,0164 %	-0,197 %	1,4201 %	17,101 %	1,4111 %	16,992 %	0,68 %	8,218 %
1,2	0,6301 %	5,564 %	3,7842 %	33,416 %	3,7481 %	33,098 %	1,78 %	15,676 %
5,8	-0,4732 %	-2,261 %	5,1571 %	24,644 %	5,0617 %	24,188 %	1,68 %	8,009 %
9	0,0000 %	0,000 %	-0,0042 %	-0,039 %	-0,0143 %	-0,133 %	-0,02 %	-0,192 %
5,8	-0,4732 %	-2,261 %	5,1571 %	24,644 %	5,0617 %	24,188 %	1,68 %	8,009 %

Figure 36: Deviations to the average method

	Base vs benchmark		Approximate vs benchmark		Timestep sum vs benchmark		Timestep prod vs benchmark	
Cut set:	Total	Weather only	Total	Weather only	Total	Weather only	Total	Weather Only
6,7	-0,9293 %	-21,390 %	-0,3013 %	-6,936 %	0,2085 %	4,798 %	0,2046 %	4,710 %
2,6	-0,9995 %	-15,743 %	-0,5714 %	-9,000 %	0,3900 %	6,144 %	0,3783 %	5,958 %
1,7	-1,3462 %	-12,571 %	-0,8165 %	-7,625 %	1,0768 %	10,055 %	1,0609 %	9,907 %
1,6	-0,6779 %	-7,594 %	-0,6941 %	-7,776 %	0,7327 %	8,208 %	0,7237 %	8,108 %
1,2	-1,7442 %	-13,551 %	-1,1251 %	-8,741 %	1,9740 %	15,337 %	1,9386 %	15,062 %
5,8	-1,6485 %	-7,415 %	-2,1139 %	-9,509 %	3,4236 %	15,401 %	3,3298 %	14,979 %
9	0,0206 %	0,192 %	0,0206 %	0,192 %	0,0165 %	0,153 %	0,0063 %	0,059 %
5,8	-1,6485 %	-7,415 %	-2,1139 %	-9,509 %	3,4236 %	15,401 %	3,3298 %	14,979 %

Figure 37: Deviations to the benchmark method

7.2 contingency analysis results

Component out matrix must be included as input without the header.

Line 1	Line 2	Line 3	LIne 4	Line 5	Line 6	Line 7	Line 8	Line 9
0	0	0	0	0	0	0	0	1
0	0	0	0	0	0	0	1	1
0	0	0	0	0	0	1	0	1
0	0	0	0	0	1	0	0	1
0	0	0	0	0	1	1	0	0
0	0	0	0	1	0	0	0	1
0	0	0	0	1	0	0	1	0
0	0	0	1	0	0	0	0	1
0	0	1	0	0	0	0	0	1
0	1	0	0	0	0	0	0	1
0	1	0	0	0	1	0	0	0
1	0	0	0	0	0	0	0	1
1	0	0	0	0	0	1	0	0
1	0	0	0	0	1	0	0	0
1	1	0	0	0	0	0	0	0

Table 25: Component out matrix

The SAC matrix must be included with the header, as the code removes the first two rows. OS is Operational State, where only one is included in this thesis. DP is Delivery Point.

OS1	OS1	OS1	OS1	OS1
DP 1	DP 2	DP 3	DP4	DP5
Inf	Inf	Inf	Inf	0
Inf	Inf	Inf	Inf	0
Inf	Inf	Inf	Inf	0
Inf	Inf	Inf	Inf	0
Inf	67,8448275862068	Inf	Inf	Inf
Inf	Inf	Inf	Inf	0
Inf	Inf	Inf	0	0
Inf	Inf	Inf	Inf	0
Inf	Inf	Inf	Inf	0
Inf	Inf	Inf	Inf	0
Inf	67,8448275862069	Inf	Inf	Inf
Inf	Inf	Inf	Inf	0
Inf	67,8448275862068	Inf	Inf	Inf
Inf	61,9999999999996	Inf	Inf	Inf
Inf	67,8448275862069	Inf	Inf	Inf

7.3 Reproduction of [1]

F	λ_{approx}	Benchmark	Deviation
0	0,00698	0,00691	1 %
10	0,00822	0,00846	-3 %
20	0,01263	0,01366	-8 %
30	0,02017	0,02247	-10 %
40	0,03083	0,03488	-12 %
50	0,04459	0,05085	-12 %
60	0,06144	0,07036	-13 %
70	0,08135	0,09338	-13 %
80	0,10430	0,11988	-13 %
90	0,13029	0,14985	-13 %
100	0,15929	0,18325	-13 %

Table 26: Duration method approximate failure rate results.

7.4 Timestep method

Figure 38 shows the unavailability of the time-series of line 9 when using the timestep method and the benchmark method. The blue line, here called Line 9 - Rolling shows the timestep method results. The red line shows the benchmark results.

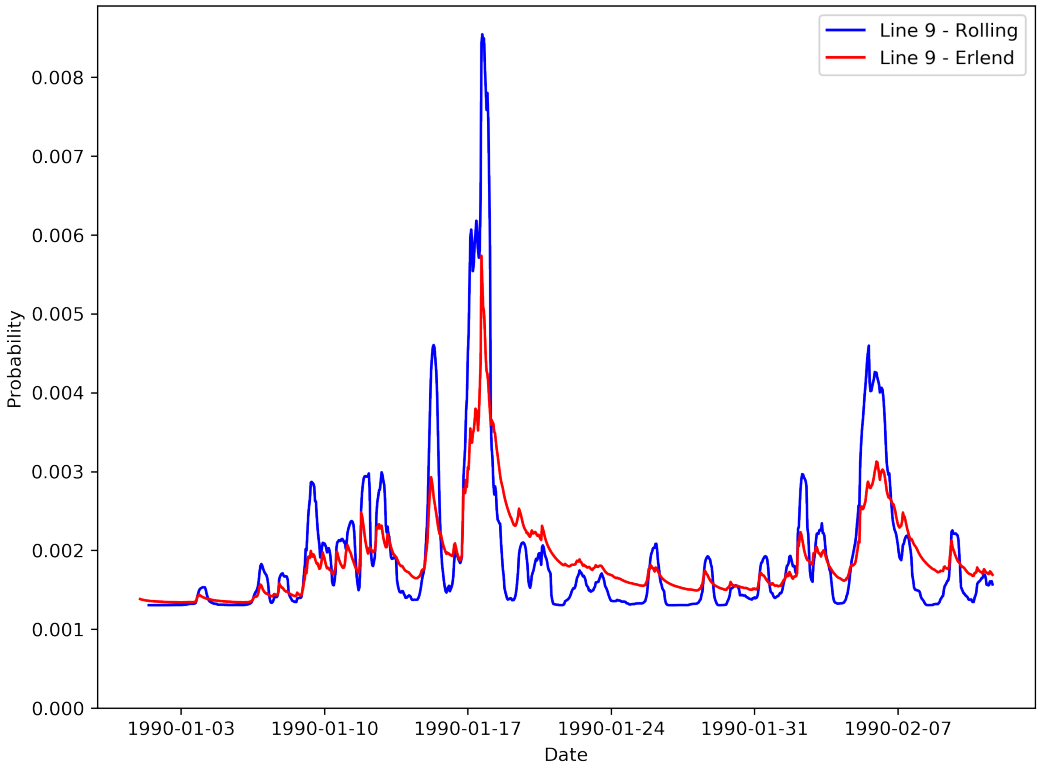

Figure 38: Line 9 unavailability for timestep vs benchmark method (By Erlend Sandø Kiel)

7.5 MATLAB Implementation

In the following section some of the most central scripts from the MATLAB implementation is added. Due to the large volume of code, not all is included. The zip file with all developed code is submitted with this thesis.

7.5.1 Main.m

```
%Only one method can be run simultanuosly.
%If the approximate equations method - approx = 1
%If base case method with no weather is wanted all parameters = 0
%If Average method is wanted - weather = 1
%If timestep sum method is wanted - timestep = 1
```

```
%If timestep product method is wanted - timestep = 1 and prod = 1


approx = 0;
weather = 0;
print_sets = 1;
print_annual = 0;
timestep=1;
prod = 1;

%Check that only one method is run:
num_method = approx + weather + timestep;

if num_method > 1
    disp('Only one method can be run at a time. Try again')
    return
end

P_n = 0.989875;
P_a = 0.010011;
P_e = 0.000114;

%Loads results of the contingency analysis
load('RBTS_cont_results.mat');
demand = [20,85,40,20,20];
lambda_rbts = [1.5,5,4,1,1,1.5,5,1,1];
r = 11.420898198198216;



%Finds minimal cut sets for each load point
cut_sets=LP_cutsets(cont_results,demand);

%If approximate equations method is chosen:
```

```
40 if approx
41     %Find transition rates from inputdata:
42     [trans_rates,lambda_avg,all_durations] = transition_rates(P_n,P_a,
           P_e);
43     %Find approximate failure rate at each cut set:
44     lambda_approx = find_approx_lambda(cut_sets,trans_rates,lambda_avg,
           P_n,P_a,P_e,lambda_rbts,all_durations);
45     %Calculate equivalent values at each cut set:
46     approx_eq_values = approx_equivalents(cut_sets,cont_results,
           lambda_approx,demand);
47     %Calculate indices for each cut set:
48     cut_set_res = cut_set_indices(approx_eq_values);
49
50 %If the OPAL methodology is chosen:
51 else
52     if weather
53         eq_values = equivalents_weather(cut_sets,cont_results,
               lambda_rbts,demand);
54         cut_set_res = cut_set_indices(eq_values);
55     else
56         %Calculates equivalent values at each cut set:
57         eq_values = equivalents(cut_sets,cont_results,lambda_rbts,
               demand);
58         %Calculates indices at each cut set:
59         cut_set_res = cut_set_indices(eq_values);
60     end
61 end
62
63 if timestep
64     flines = csvread('f_lines_rbts.csv',1,1);
65     years = size(flines,1)/8760;
66     if prod
67         cut_set_res = timestep_prod(cut_sets,flines,years,cont_results,
               demand,lambda_rbts,r);
```

```
68      else
69          cut_set_res = timestep_sum(cut_sets,flines,years,cont_results,
                demand,lambda_rbts,r);
70      end
71
72      annual_res = annual_indices_timestep(cut_set_res);
73
74  else
75  %Calculates annual results at each load point:
76  annual_res = annual_indices(cut_set_res);
77
78  end
79  %Prints cut set indices if chosen:
80  if print_sets
81      write_cut_set_indices(cut_set_res);
82  end
83
84  %Prints annual load point indices if chosen:
85  if print_annual
86      write_annual_indices(annual_res);
87  end
```

7.5.2 *LP_cutsets.m*

```
function cutsets = LP_cutsets(cont_results,demand)

    %Retrieve necessary variables from the contingency analysis:
    SAC=cont_results.SAC(3:end,1:end);
    comp_out=full(cont_results.comp_out);
    cutsets=struct;

    %Loop through all load points:
    for i = 1:size(SAC,2)
        load_point =strcat('load',num2str(i));
        load = struct;
        sets= {};
        SAC_id={};

        %Loop through every fault combination:
        for j = 1:size(SAC,1)

            %Check if there is loss of load:
            if demand(i) > SAC(j,i)

                %Find components in the cut set and add at the end of
                    the
                %cell "sets":
                sets{end+1} = find(comp_out(j,:));
                SAC_id{end+1} = j;
            end
        end

        %If a load point has no loss of load. Add to struct:
        if isempty(sets)
            cutsets = setfield(cutsets,load_point,{});
            continue
```

```
32          end
33
34          %check if any cut set is not minimal:
35          combinations =  combnk([1:length(sets)],2);  %every possible
               combination
36          index = ones(length(sets),1);
37
38             %Loops thorough every combination of cut sets to check if a
                  cut
39             %set is a sub set of another cut set:
40             for k = 1:length(combinations)
41                  set_1 = sets{combinations(k,1)};
42                  set_2 = sets{combinations(k,2)};
43                      if length(set_1) < length(set_2)
44                          shortest= set_1;
45                          longest = set_2 ;
46                          id=combinations(k,2);
47                      else
48                          shortest=set_2;
49                          longest = set_1;
50                          id=combinations(k,1);
51                      end
52                  %Checks if the shortest subset is a subset of the
                       longest
53                  %subset. (f.eks 1. order contingency is a subset of the
54                  %cut set of a 2. order contingency:
55                  a = ismember(shortest,longest);
56                      if  sum(a) == length(a)
57                           index(id) = 0;
58                      end
59             end
60
61             %Removes all sets that are not minimal:
62             min_cut = sets(index == 1);
```

```
63              SAC_id = SAC_id(index==1);
64
65              %Adds results to load struct.
66              load = setfield(load,'min_cut',min_cut);
67              load = setfield(load, 'SAC_id' , SAC_id);
68
69              %Add load struct to cut sets struct
70              cutsets = setfield(cutsets,load_point,load);
71      end
72
73  end
```

7.5.3 *find_approx_lambda.m*

```
function lambda_approx = find_approx_lambda(cut_sets,trans_rates,
    lambda_avg,P_n,P_a,P_e,lambda_rbts,all_durations)

    %Defines necessary data structure:
    cut_sets = struct2cell(cut_sets);
    lambda_approx = struct;

    %Loops through each load point:
    for i = 1:length(cut_sets)
        load_point =strcat('load',num2str(i));
        sets = {};
        %If no loss of load at load point, keep empty:
        if isempty(cut_sets{i})
            lambda_approx = setfield(lambda_approx,load_point,{});
            continue
        end

        min_cut = cut_sets{i}.min_cut;
        %Loop through each minimal cut set:
        for j = 1:length(min_cut)
            %First order minimal cut set:
            if length(min_cut{j}) == 1
                sets{j}.lambda = lambda_rbts(min_cut{j}(1))+ P_n*
                    lambda_avg{j}(1)*8760 + P_a*lambda_avg{j}(2)*8760 +
                    P_e*lambda_avg{j}(3)*8760;
                sets{j}.set = min_cut{j};
            %Second order minimal cut set:
            else
                sets{j}.lambda = three_state_approx(min_cut{j}(1),
                    min_cut{j}(2),trans_rates,lambda_avg,P_n,P_a,P_e,
                    lambda_rbts,all_durations);
                sets{j}.set = min_cut{j};
```

```
28              end
29          end
30          %Add results to struct:
31          lambda_approx = setfield(lambda_approx,load_point,sets);
32      end
33
34
35
36  end
```

7.5.4 *three_state_approx.m*

```
function lambda_approx = three_state_approx(line_1,line_2,trans_rates,
    lambda_avg,p_n,p_a,p_e,lambda_rbts,all_durations)

    %Define failure rate for both lines for all weather states:
    lambda_n_1 = lambda_rbts(line_1) + lambda_avg{line_1}(1)*8760;
    lambda_n_2 = lambda_rbts(line_2) + lambda_avg{line_2}(1)*8760;
    lambda_a_1 = lambda_rbts(line_1) + lambda_avg{line_1}(2)*8760;
    lambda_a_2 = lambda_rbts(line_2) + lambda_avg{line_2}(2)*8760;
    lambda_e_1 = lambda_rbts(line_1) + lambda_avg{line_1}(3)*8760;
    lambda_e_2 = lambda_rbts(line_2) + lambda_avg{line_2}(3)*8760;

    %Set expected repair time:
    r_1 = 11.420898198198216/8760;
    r_2 = 11.420898198198216/8760;


    %Define all possible transition rates:
    n_a_1 = trans_rates{line_1}(1,2);
    n_a_2 = trans_rates{line_2}(1,2);
    n_e_1 = trans_rates{line_1}(1,3);
    n_e_2 = trans_rates{line_2}(1,3);
    a_n_1 = trans_rates{line_1}(2,1);
    a_n_2 = trans_rates{line_2}(2,1);
    a_e_1 = trans_rates{line_1}(2,3);
    a_e_2 = trans_rates{line_2}(2,3);
    e_n_1 = trans_rates{line_1}(3,1);
    e_n_2 = trans_rates{line_2}(3,1);
    e_a_1 = trans_rates{line_1}(3,2);
    e_a_2 = trans_rates{line_2}(3,2);

%The following part calculates transition rates for each transition and
%takes into account if one or both are zero:
```

```
32
33      %From Normal to Adverse
34      if n_a_1 == 0 && n_a_2 == 0
35          disp('no transition on n_a');
36          n_a = 0;
37      elseif n_a_1 == 0
38          n_a = n_a_2;
39      elseif n_a_2 == 0
40          n_a = n_a_1   ;
41      else
42          n_a = ((n_a_1 + n_a_2)/2);
43      end
44
45      %From Normal to Extreme:
46      if n_e_1 == 0 && n_e_2 == 0
47          disp('no transition on n_e');
48          n_e = 0;
49      elseif n_e_1 == 0
50          n_e = n_e_2;
51      elseif n_e_2 == 0
52          n_e = n_e_1;
53      else
54      n_e = ((n_e_1 + n_e_2)/2);
55      end
56
57
58      %From Adverse to Normal
59      if a_n_1 == 0 && a_n_2 == 0
60          disp('no transition on a_n');
61          a_n = 0;
62      elseif a_n_1 == 0
63          a_n = a_n_2   ;
64      elseif a_n_2 == 0
65          a_n = a_n_1   ;
```

```
66      else
67          a_n = ((a_n_1 + a_n_2)/2);
68      end
69
70      %From Adverse to Extreme:
71      if a_e_1 == 0 && a_e_2 == 0
72          disp('no transition on a_e');
73          a_e = 0;
74      elseif a_e_1 == 0
75          a_e = a_e_2 ;
76      elseif a_e_2 == 0
77          a_e = a_e_1 ;
78      else
79          a_e = ((a_e_1 + a_e_2)/2) ;
80      end
81
82      %From Extreme to normal:
83      if e_n_1 == 0 && e_n_2 == 0
84          disp('no transition on e_n');
85          e_n = 0;
86      elseif e_n_1 == 0
87          e_n = e_n_2 ;
88      elseif e_n_2 == 0
89          e_n = e_n_1 ;
90      else
91          e_n = ((e_n_1 + e_n_2)/2) ;
92      end
93
94
95
96      %From Extreme to Adverse:
97      if e_a_1 == 0 && e_a_2 == 0
98          disp('no transition on n_a');
99          e_a = 0;
```

```
100     elseif e_a_1 == 0
101         e_a = e_a_2    ;
102     elseif e_a_2 == 0
103         e_a = e_a_1 ;
104     else
105         e_a = ((e_a_1 + e_a_2)/2) ;
106     end
107
108
109
110     %Calculates weather durations:
111     N = ((sum(all_durations{line_1}{1,2}) + sum(all_durations{line_1
            }{1,3}) + sum(all_durations{line_2}{1,2}) + sum(all_durations{
            line_2}{1,3})) ...
112          / (length(all_durations{line_1}{1,2}) + length(all_durations{
                line_1}{1,3}) + length(all_durations{line_2}{1,2}) + length(
                all_durations{line_2}{1,3})))/8760;
113
114     A = ((sum(all_durations{line_1}{2,1}) + sum(all_durations{line_1
            }{2,3}) + sum(all_durations{line_2}{2,1}) + sum(all_durations{
            line_2}{2,3})) ...
115          / (length(all_durations{line_1}{2,1}) + length(all_durations{
                line_1}{2,3}) + length(all_durations{line_2}{2,1}) + length(
                all_durations{line_2}{2,3})))/8760;
116
117     E = ((sum(all_durations{line_1}{3,1}) + sum(all_durations{line_1
            }{3,2}) + sum(all_durations{line_2}{3,1}) + sum(all_durations{
            line_2}{3,2})) ...
118          / (length(all_durations{line_1}{3,1}) + length(all_durations{
                line_1}{3,2}) + length(all_durations{line_2}{3,1}) + length(
                all_durations{line_2}{3,2})))/8760;
119
120     %Both failures occur in normal weather:
121     lambda_1 = p_n*(lambda_n_1*(1-exp(-lambda_n_2*r_1)) + lambda_n_2
```

```
    *(1-exp(-lambda_n_1*r_2)));
122
123     %First failure in normal, second in adverse:
124     lambda_2 = p_n*(lambda_n_1*(1-exp(-n_a*r_1))*exp(-lambda_n_2*r_1)
            *(1-exp(-lambda_a_2*A))...
125     + lambda_n_2*(1-exp(-n_a*r_2))*exp(-lambda_n_1*r_2)*(1-exp(-
            lambda_a_1*A)));
126
127     %First failure in normal, second in extreme:
128     lambda_3 = p_n*(lambda_n_1*(1-exp(-n_e*r_1))*exp(-lambda_n_2*r_1)
            *(1-exp(-lambda_e_2*E))...
129     + lambda_n_2*(1-exp(-n_e*r_2))*exp(-lambda_n_1*r_2)*(1-exp(-
            lambda_e_1*E)));
130
131     %First failure in adverse, second in  normal:
132     lambda_4 = p_a*(lambda_a_1*(1-exp(-a_n*A))*exp(-lambda_a_2*A)*(1-
            exp(-lambda_n_2*r_1))...
133     + lambda_a_2*(1-exp(-a_n*A))*exp(-lambda_a_1*A)*(1-exp(-lambda_n_1*
            r_2)));
134
135     %Both failure in adverse:
136     lambda_5 = p_a*(lambda_a_1*(1-exp(-lambda_a_2*A)) + lambda_a_2*(1-
            exp(-lambda_a_1*A)));
137
138
139     %First failure in adverse, second in extreme:
140     lambda_6 = p_a*(lambda_a_1*(1-exp(-a_e*A))*exp(-lambda_a_2*A)*(1-
            exp(-lambda_e_2*E))...
141     + lambda_a_2*(1-exp(-a_e*A))*exp(-lambda_a_1*A)*(1-exp(-lambda_e_1*
            E)));
142
143
144     %First failure in extreme, second in normal:
145     lambda_7 = p_e*(lambda_e_1*(1-exp(-e_n*E))*exp(-lambda_e_2*E)*(1-
```

```
        exp(-lambda_n_2*r_1)) ...
146     + lambda_e_2*(1-exp(-e_n*E))*exp(-lambda_e_1*E)*(1-exp(-lambda_n_1*
            r_2)));
147
148
149     %First failure in extreme, second in adverse:
150     lambda_8 = p_e*(lambda_e_1*(1-exp(-e_a*E))*exp(-lambda_e_2*E)*(1-
            exp(-lambda_a_2*A)) ...
151     + lambda_e_2*(1-exp(-e_a*E))*exp(-lambda_e_1*E)*(1-exp(-lambda_a_1*
            A)));
152
153     %Both failure occur in extreme weather:
154     lambda_9 = p_e*(lambda_e_1*(1-exp(-lambda_e_2*E)) + lambda_e_2*(1-
            exp(-lambda_e_1*E)));
155
156     %Calculates approximate failure rate for the system:
157     lambda_approx = lambda_1 + lambda_2 + lambda_3 + lambda_4 +
            lambda_5 + lambda_6 + lambda_7 + lambda_8 + lambda_9;
158
159     lambda = [lambda_1,lambda_2,lambda_3 ; lambda_4,lambda_5,lambda_6 ;
             lambda_7,lambda_8,lambda_9];
160
161 end
```

7.5.5 *timestep_sum.m*

```
function cut_set_res = timestep_sum(cut_sets,f_prob,years,cont_results,
    demand,lambda_rbts,r)


    cut_sets = struct2cell(cut_sets);
    SAC = cont_results.SAC(3:end,1:end);
    conv_fprob = conv2(ones(11,1),1,f_prob,'valid');
    cut_set_res = struct;

    %Loops through each load point
    for i = 1:size(SAC,2)
        load = {};
        load_point =strcat('load',num2str(i));

        %If no loss of load at load point, keep empty.
        if isempty(cut_sets{i})
            cut_set_res = setfield(cut_set_res,load_point,{});
            continue
        end

        %Retrieve minimal cut sets from input:
        min_cuts = cut_sets{i}.min_cut;
        SAC_id = cut_sets{i}.SAC_id;

        %Loops through each minimal cut set:
        for j = 1:length(min_cuts) %each cut set
          sets=struct;
            P_int = demand(i)-SAC(SAC_id{j},i);
            comp = min_cuts{j};
            U_sum=0;
            w=r/11;

```

```
32              %If first order minimal cut set:
33              if length(comp) == 1
34                      U_rbts_1 = lambda_rbts(comp(1))*r/8760;
35                      for k = 1:size(conv_fprob,1)
36                          U_sum = U_sum + (U_rbts_1 +(conv_fprob(k,comp
                                (1)))*w);
37                      end
38
39              %Second order minimal cut set:
40              else
41                  U_rbts_1 = lambda_rbts(comp(1))*r/8760;
42                  U_rbts_2 = lambda_rbts(comp(2))*r/8760;
43                 %Calculates U at each timestep
44                  for k = 1:size(conv_fprob,1)
45                      U_sum = U_sum + (U_rbts_1 +(conv_fprob(k,comp(1)))*
                            w)*(U_rbts_2 + (conv_fprob(k,comp(2)))*w);
46                  end
47              end
48
49              %Calculates yearly indices:
50              U_eq = U_sum/years;
51              ENS = U_eq * P_int;
52              %Defines indicies in the struct:
53              sets.cut = comp;
54              sets.U_eq = U_eq;
55              sets.ENS = ENS;
56              sets.P_int = P_int;
57              load{end + 1} = sets;
58          end
59          cut_set_res = setfield(cut_set_res,load_point,load);
60      end
61
62  end
```

7.5.6 equivalents.m

```
1
2  function eq_values =  equivalents(cut_sets,cont_results,lambda_rbts,
       demand)
3
4     %RBTS har kun parallelle minimale kuttesett, og det er kun dette som
          er
5     %inkludert i denne utregningen
6
7      %Retrieve neccesary data from the contingency analysis.
8
9      r = 11.420898198198216;
10     cut_sets = struct2cell(cut_sets);
11     eq_values = struct;
12     comp_out = full(cont_results.comp_out);
13     SAC = cont_results.SAC(3:end,1:end);
14
15     %Loops through all load points:
16     for i = 1:size(cut_sets,1)
17             load_point =strcat('load',num2str(i));
18             load={};
19             P_int = 0;
20             lambda_eq = 0;
21             r_eq = 0;
22             U_eq = 0;
23
24            %Adds load points with no loss of load to struct.
25            if isempty(cut_sets{i})
26                eq_values = setfield(eq_values,load_point,{});
27                continue
28            end
29
30            %Retrieve minimal cut sets from input:
```

```
31              min_cuts = cut_sets{i}.min_cut;
32              SAC_id = cut_sets{i}.SAC_id;
33
34              %Loops through every minimal cut set
35              for j = 1:size(SAC_id,2)
36                      sets = struct;
37                      comp = min_cuts{j} ;
38                      P_int = demand(i) - SAC(SAC_id{j},i);
39
40
41                      % 1. order minimal cut:
42                      if length(comp) == 1
43                          lambda_eq = lambda_rbts(comp(1));
44                          r_eq = r;
45                          U_eq = lambda_eq * r_eq;
46
47                      % 2. order minimal cut:
48                      else
49                           lambda_1 = lambda_rbts(comp(1));
50                           lambda_2 = lambda_rbts(comp(2));
51                           lambda_eq = (lambda_1 * lambda_2 * (r + r))
                                 /(8760 + lambda_1*r + lambda_2*r);
52                           r_eq = (r * r)/(r + r) ;
53                           U_eq = lambda_eq * r_eq;
54
55
56                     %Adds results to the sets struct
57                      sets.P_int = P_int;
58                      sets.lambda_eq=lambda_eq;
59                      sets.r_eq = r_eq;
60                      sets.U_eq = U_eq;
61                      sets.set= comp;
62
63                     %Adds sets to the load cell
```

```
64                      load{end+1} = sets;
65                  end
66
67                  %Adds the load cell to the eq_values struct
68                  eq_values = setfield(eq_values,load_point,load);
69
70          end
71
72
73  end
```

7.5.7 *cut_set_indices.m*

```
function cut_set_res = cut_set_indices(eq_values)

    %Calculates ENS for each minimal cut set
    %Only one operational state is included

    %Retrieves cut set parameters in a cell structure:
    cut_set = struct2cell(eq_values) ;

    %Loops through every load point:
    for i = 1:length(cut_set)


        %If no loss of load at load point, keep empty.
        if isempty(cut_set(i))
            continue
        end

        %Loops through every minimal cut set:
        for j = 1:size(cut_set{i},2)

            %Retrieves known parameters from cut set:
            P_int = cut_set{i}{j}.P_int ;
            lambda_eq = cut_set{i}{j}.lambda_eq ;
            r_eq = cut_set{i}{j}.r_eq;

            %Calculates indices:
            ENS = lambda_eq * r_eq * P_int ; %[MWh/year]
            P_int_c = P_int*lambda_eq;

            %Includes calculated indices to results:
            cut_set{i}{j}.ENS = ENS;
            cut_set{i}{j}.P_int_c = P_int_c ;
```

```
33
34          end
35
36      end
37
38      %Returns results to struct and names each loadpoint:
39      cut_set_res = cell2struct(cut_set(1:5),{'Load1','Load2','Load3','
            Load4','Load5'},1);
40
41  end
```

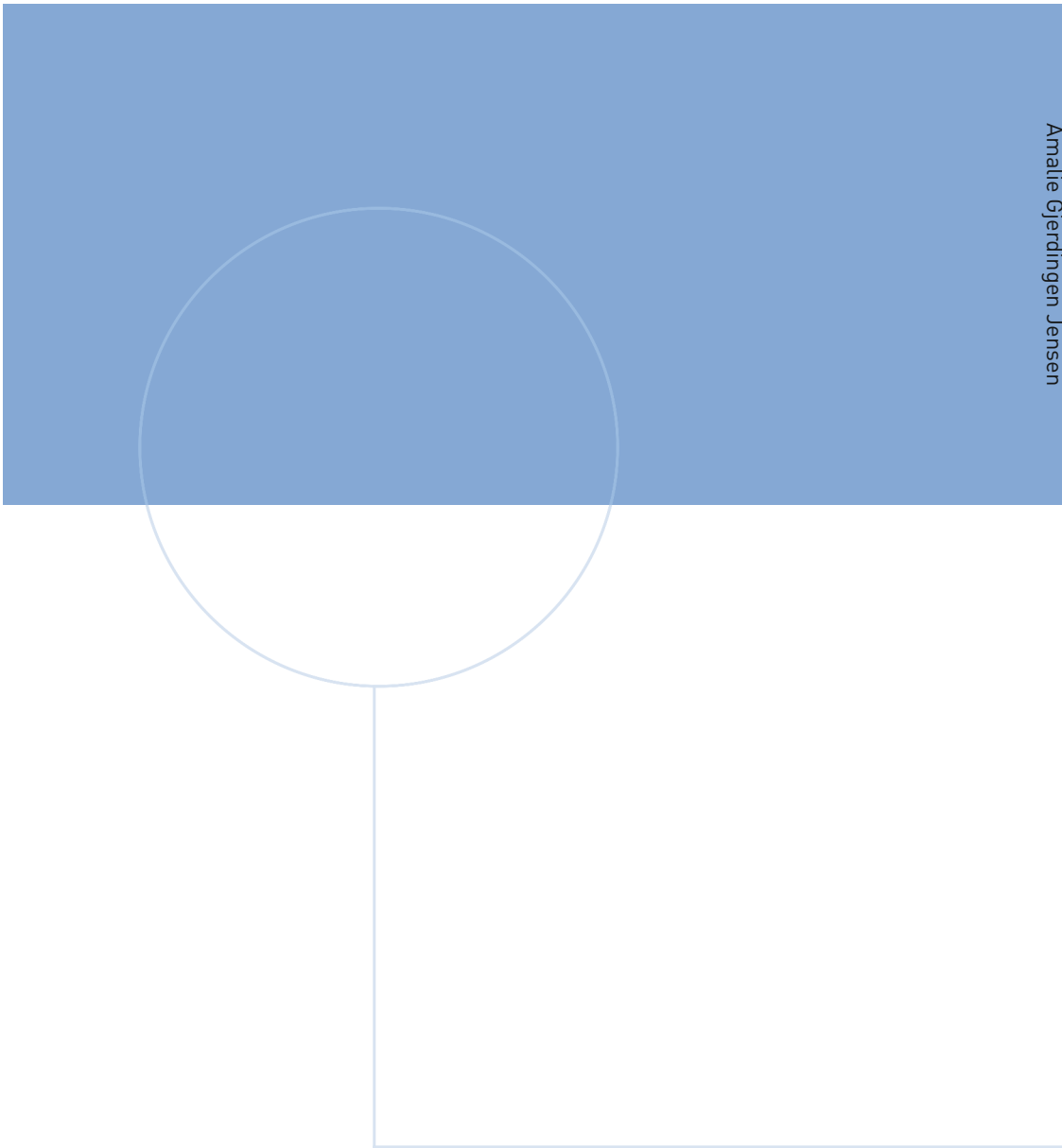

Amalie Gjerdingen Jensen

NTNU
Norwegian University of
Science and Technology